New developments in NWChem applied to the calculation of defects in fusion materials

Eric J. Bylaska[1], Fei Gao[1], Kir
and Marat Valie

[1] Pacific Northwest Nationa
[2] Department of Chemistry, Unive

Pacific Northwest National Laboratory
Operated by Battelle for the U.S. Department of Energy

Battelle

Outline

- Defect calculations of silicon carbide
- Characterizing the electronic states of large electronic structure calculations
- New developments in the plane-wave modules in NWChem
  1. Self interaction corrections
  2. Exact exchange and preliminary results on Hybrid functionals (e.g. B3LYP)
- Conclusions

NWPW Modules of NWChem

Three modules are available to compute the energy, optimize the geometry, numerical second derivatives, and perform ab initio molecular dynamics using pseudopotential plane-wave DFT.

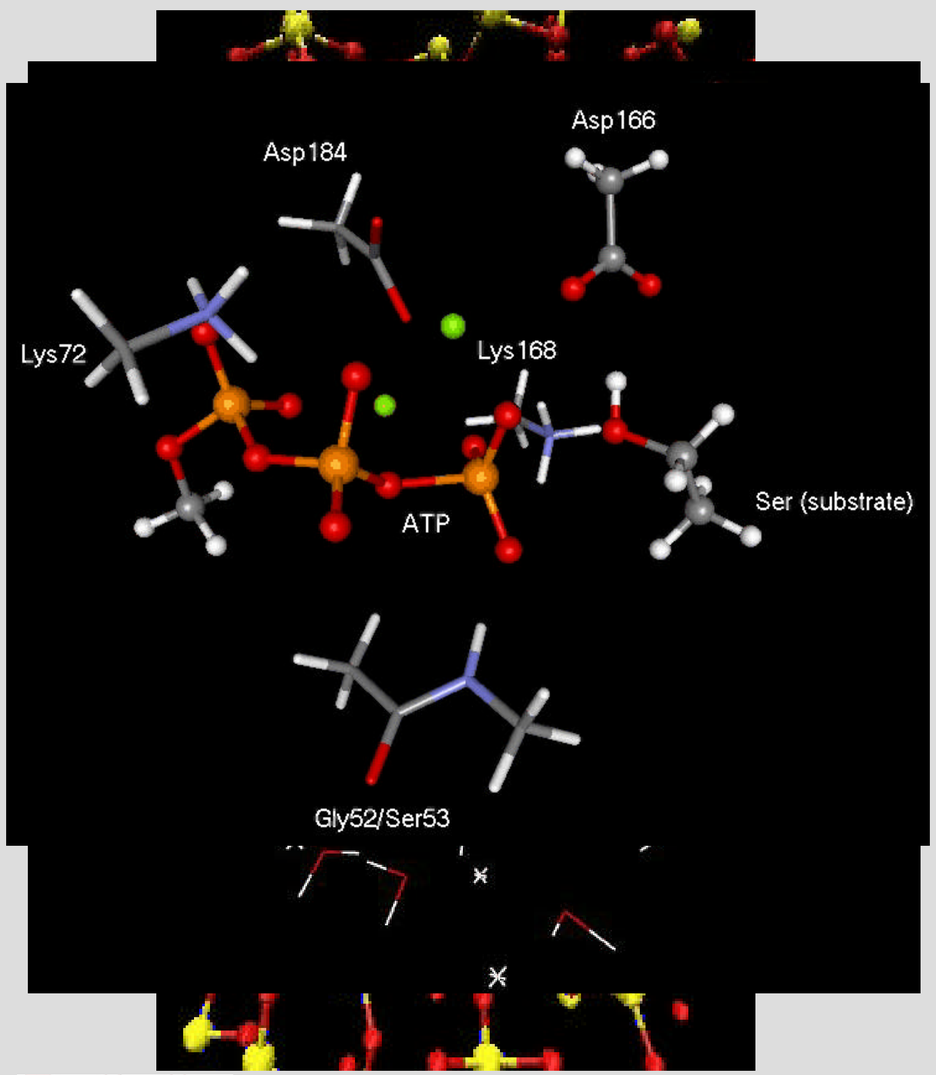

- **PSPW - (Pseudopotential plane-wave) A gamma point code for calculating molecules, liquids, crystals, and surfaces.**

- **Band - A band structure code for calculating crystals and surfaces with small band gaps (e.g. semi-conductors and metals)**

- **PAW - a gamma point projector augmented plane-wave code for calculating molecules, crystals, and surfaces**

Introduction

Silicon carbide (SiC) has been recognized as a potential cladding material for gas-cooled fission reactors, structural components for fusion reactors and an inert matrix for the transmutation of plutonium because of its small neutron capture cross section, low activation and good thermal conductivity under irradiation. In these extreme radioactive environments, bombardment by high-energy positrons, protons or neutrons result in a cascade of native and interstitial defects.

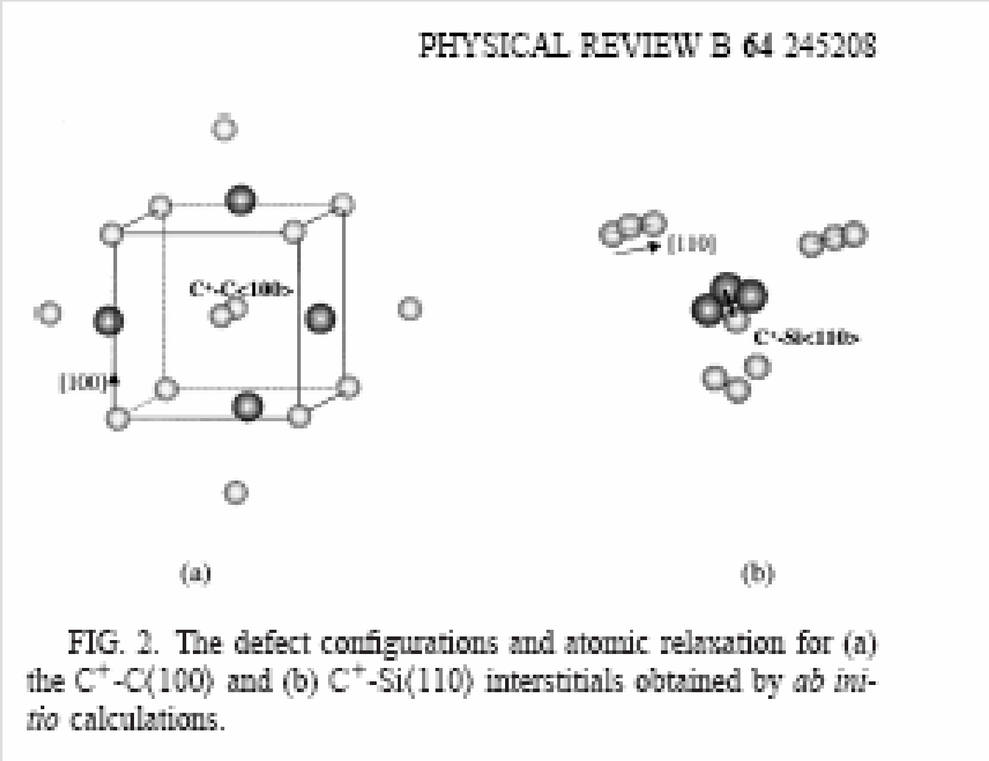

FIG. 2. The defect configurations and atomic relaxation for (a) the C^+-C⟨100⟩ and (b) C^+-Si⟨110⟩ interstitials obtained by *ab initio* calculations.

Typically, molecular dynamics (MD) simulations have been used to simulate high-energy cascades. However, a considerable amount ambiguity has been introduced into the literature regarding the formation of native defects, their clusters and in particular the stability of interstitial configurations, *because different MD potentials lead to different results.* The alternative is to use electronic structure methods, but the number of atoms needed to simulate a cascade process prohibits the use of even the most efficient of these methods.

Electronic structure calculations can provide a set of accurate defect formation energies and also guidelines for evaluating the quality and fit of empirical potentials.

Multi-scale modeling of SiC – Parameter Passing

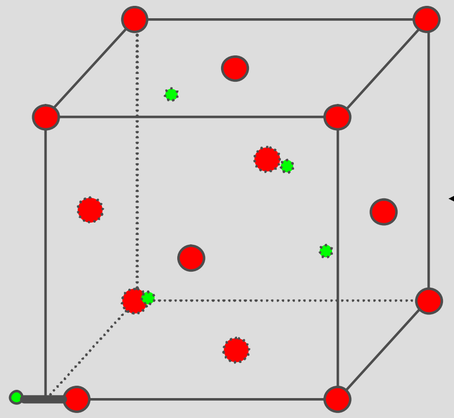

C^+-Si<100>

Defect properties

Ab initio calculations

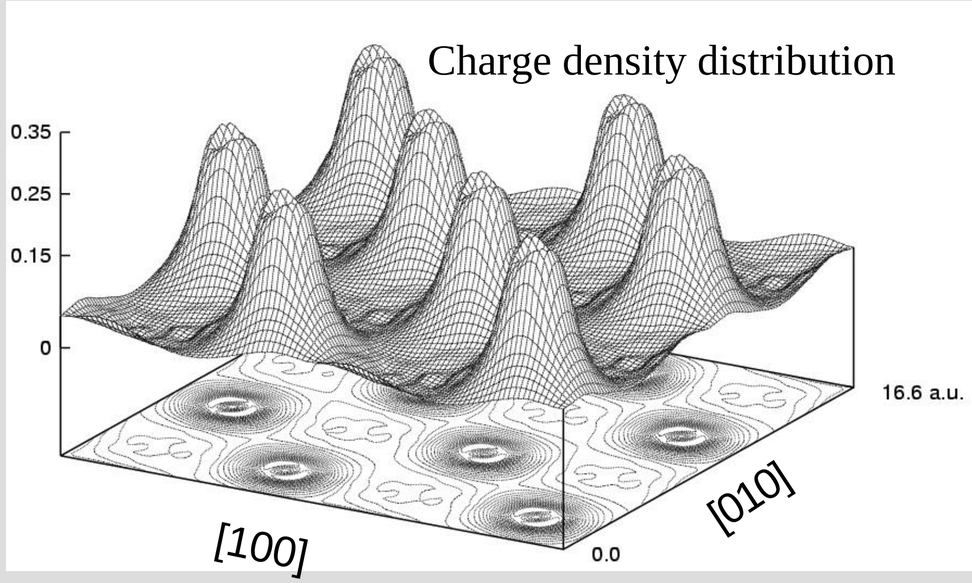

Evaluating and fitting empirical potentials

MD simulations :

Migration of point defect and clusters, binding energies and interaction of defect with dislocations

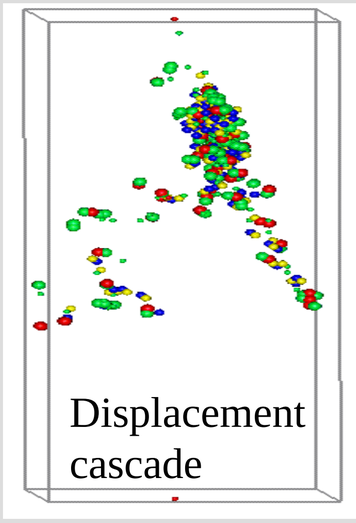

Displacement cascade

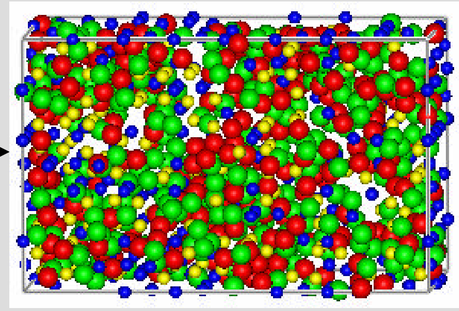

Cascade overlap

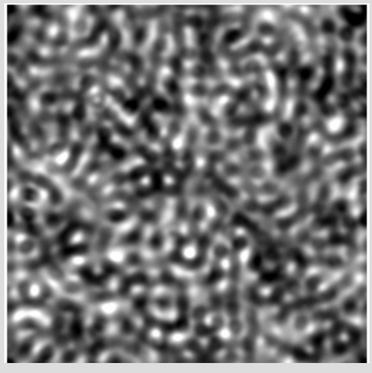

TEM images

Kinetic Monte Carlo :

Defect annealing and accumulations.

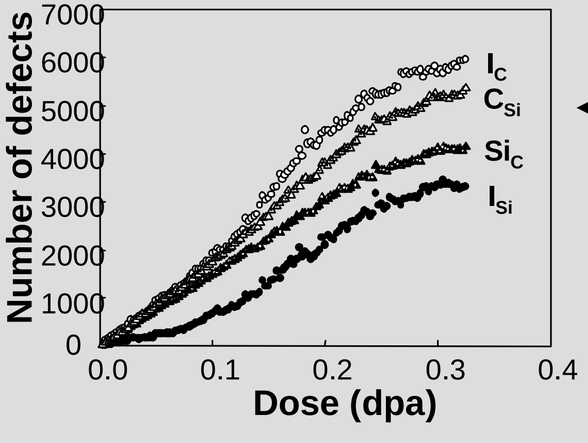

Defect accumulation

Continuum model

Experimental observations

Displacement Cascades

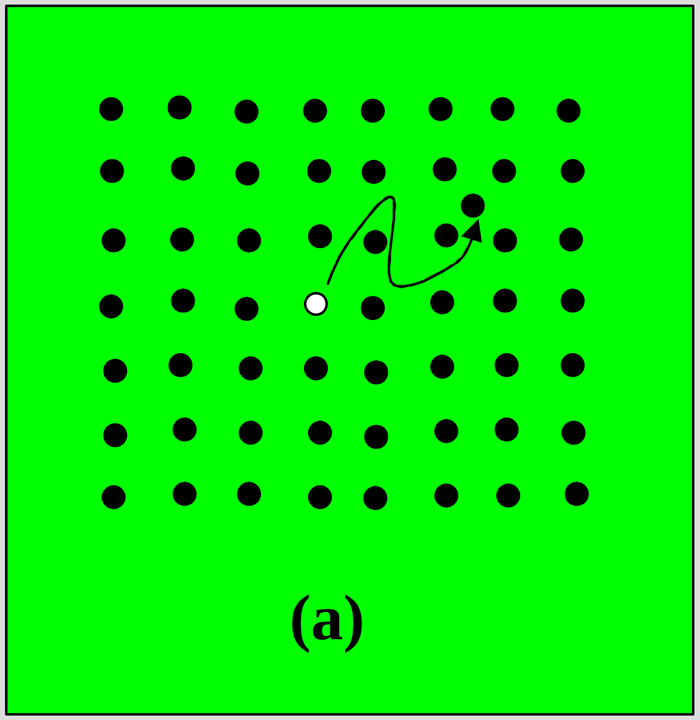

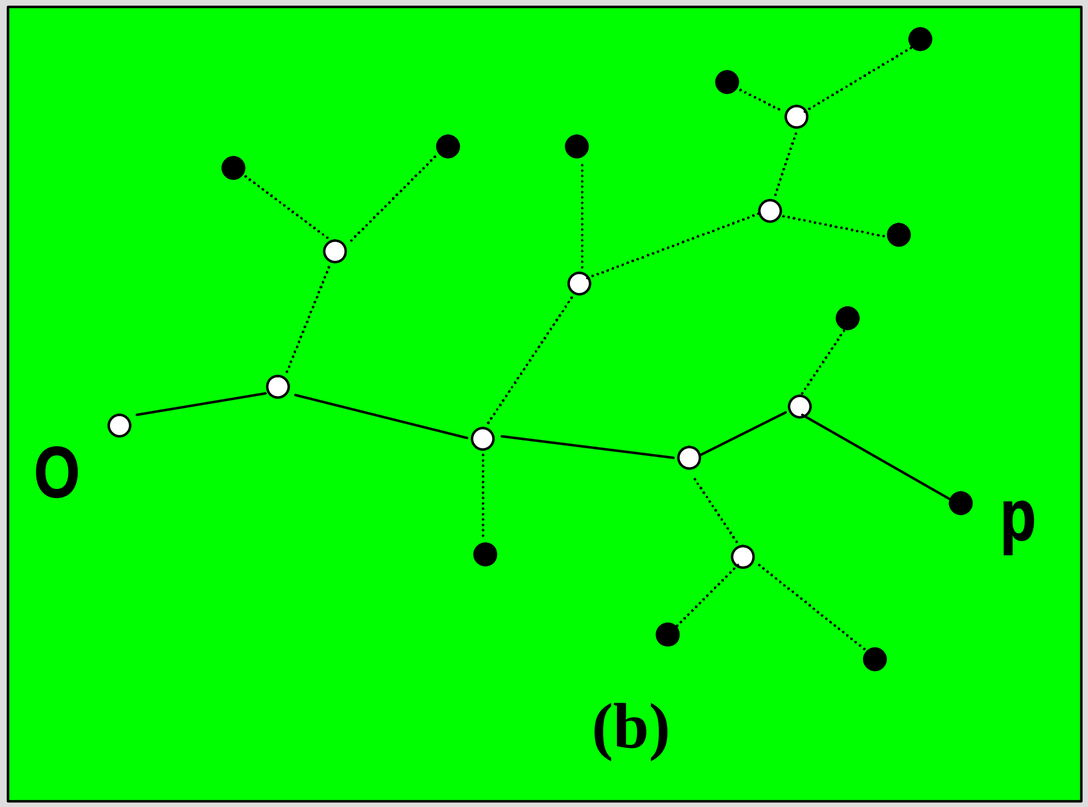

• **Interstitial** ○ **Vacancy**

a. Creation of a Frenkel pair by an elemental displacement process.

b. Schematic representation of a displacement cascade : O, starting point of the primary knock-on; p, stopping point.

Results from MD simulations of Si displacement cascades in 3C-SiC

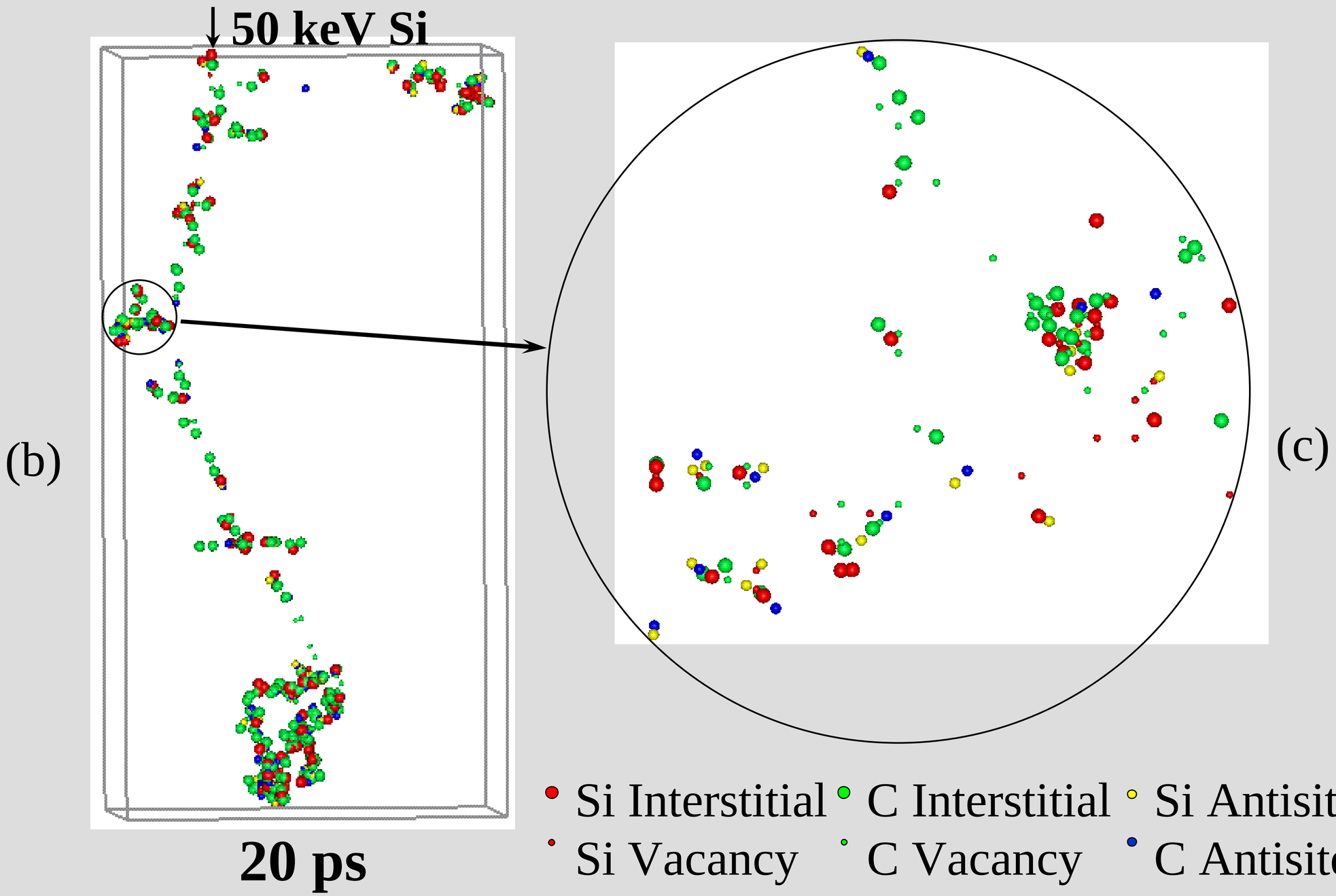

- Most defects are single interstitials and mono-vacancies.
- Only small proportion of interstitials is formed in clusters.

Defect Properties in SiC (Ab initio and MD Calculations)

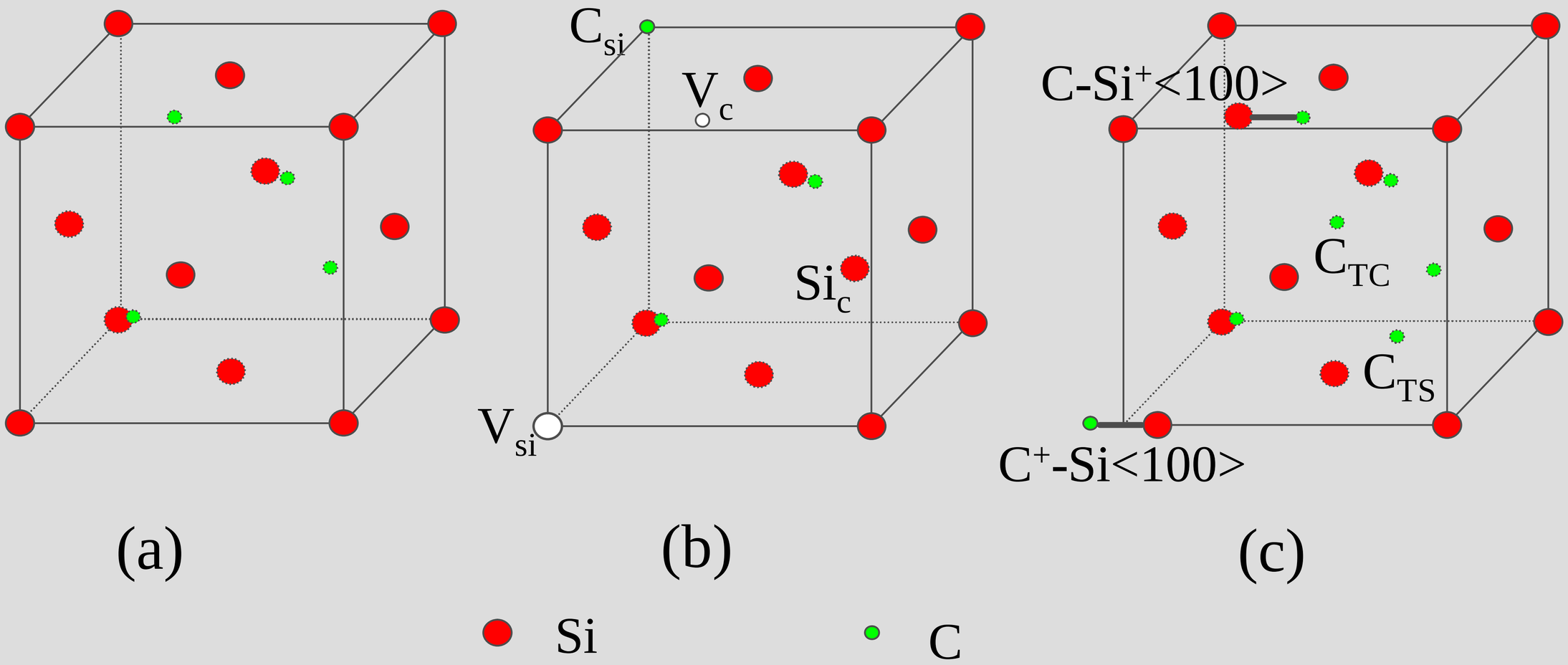

- **The possible defects :**

  V_C, V_{Si}, C_{Si} and Si_C; **C_{TS}, C_{TC}, Si_{TS} and Si_{TC};**

  C^+-Si<100>, C-Si^+<100>, C^+-C<100> and Si^+-Si<100>

Size Effects in Ab Initio Calculations

Defects	Previous First Principles (atoms in unit cell)	Present First Principles (atoms in unit cell)
V_C	5.9 (31)	5.48 (31)
V_{Si}	6.8 (31)	6.64 (31)
C_{TC}	11.0 (33)	6.41 (65)
C_{TS}	8.6 (33)	5.84 (65)
Si_{TC}	14.7 (33)	6.17 (65)
Si_{TS}	15.0 (33)	8.71 (65)
$C\text{-}Si^{+}$<100>	-	10.05 (65)
$C^{+}\text{-}Si$<100>	-	3.59 (65)
$C^{+}\text{-}C$<100>	-	3.16 (65)
$Si^{+}\text{-}Si$<100>	-	9.32 (65)
$C^{+}\text{-}C$<110>	-	3.32 (65)
$C^{+}\text{-}Si$<110>	-	3.28 (65)
C_{Si}	1.10 (32)	1.32 (32)
Si_C	7.30 (32)	7.20 (32)

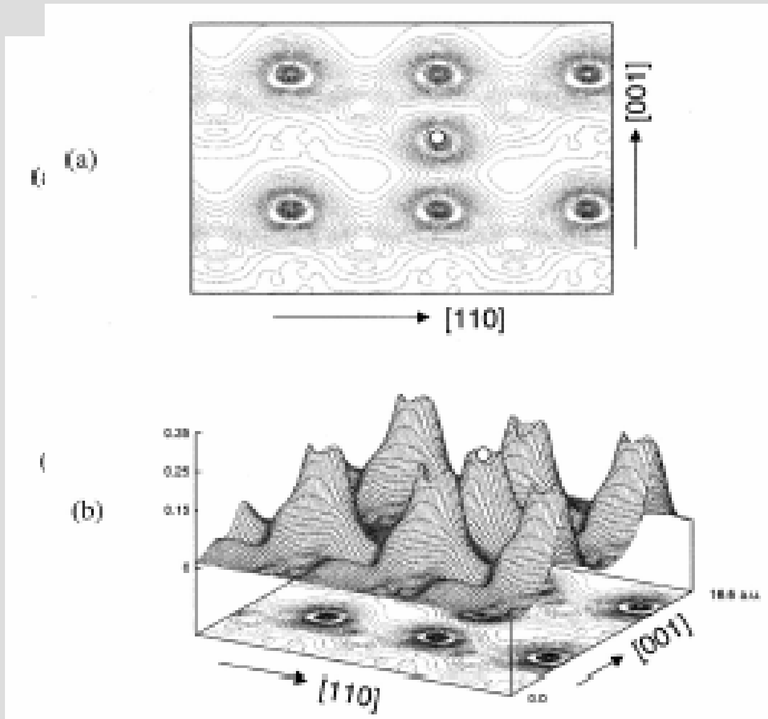

FIG. 4. (a) The charge density (a.u.) contour plot and (b) the charge density surface distribution on the $[1\bar{1}0]$ plane for the C_{TS} interstitial. The position of the interstitial is indicated by the solid circle.

- **32, 64, and 128 atom supercells**
- **Cutoff energy of 36 Ry and 82 Ry**

MP2 correction
1.5
6.9

Defect Properties in SiC (Electronic Structure and MD Calculations)

Defects	Formation energy (eV)		
	Tersoff[2]	First principles*	First principles (present work)
V_c	5.15	5.90	5.48
V_{si}	6.31	6.80	6.64
C_{Si}	0.35	1.10	1.32
Si_C	5.5	7.30	7.20
C_{TC}	8.34	11.0	6.41
C_{TS}	6.68	8.6	5.84
Si_{TC}	10.52	14.7	6.17
Si_{TS}	14.33	15.0	8.71
C^+-Si<100>	5.88	-	3.59
C-C<100>	5.97	-	3.16
C-Si^+<100>	11.28	-	10.05
Si^+-Si<100>	10.03	-	9.32
C^+-Si<110>	9.39	-	3.28
C^+-C<110>	6.50	-	3.32

- In general, the properties of vacancies and antisites are in good agreement.
- Interstitial results with Tersoff[2] are different from electronic structure results, particularly related to the stability of interstitials.

* C. Wang et al. Rhys. Rev., B 38 (1988) 12752.

New (Brenner) Potential developed based on Electronic Structure Calculations

Parameters used for fitting potentials:

- Cohesive energy, lattice constant, elastic constants, the formation energies of four C interstitials.

Results

- The equilibrium properties of bulk SiC calculated with the new potential are in good agreement with experiments.

Formation energy (eV)

Defects	Ab intio (present work)	New Potential	Tersoff[1]
C^+-C<100>	3.16	3.04	6.41
C^+-Si<100>	3.59	3.43	9.03
C^+-C<110>	3.32	3.30	6.21
C^+-Si<110>	3.28	3.95	unstable
C_{SI}	1.32 (1.5 MP2)	1.69	0.35
Si_C	7.20 (6.9 MP2)	4.12	6.1
V_c	5.48	2.76	5.20
V_{Si}	6.64	3.34	6.31
C-Si^+<100>	10.05	7.54	9.10
C_{TC}	6.41	4.65	4.86

Ab Initio Molecular Dynamics Simulation of Defect Annealing

Are neigboring antisite defects stable to high temperatures?

- MD simulations readily predict interchange
- Much longer interchange for 1500K simulations
- DFT may be predicting low barriers

SiC antisite pair Car-Parrinello simulation, T=2000K

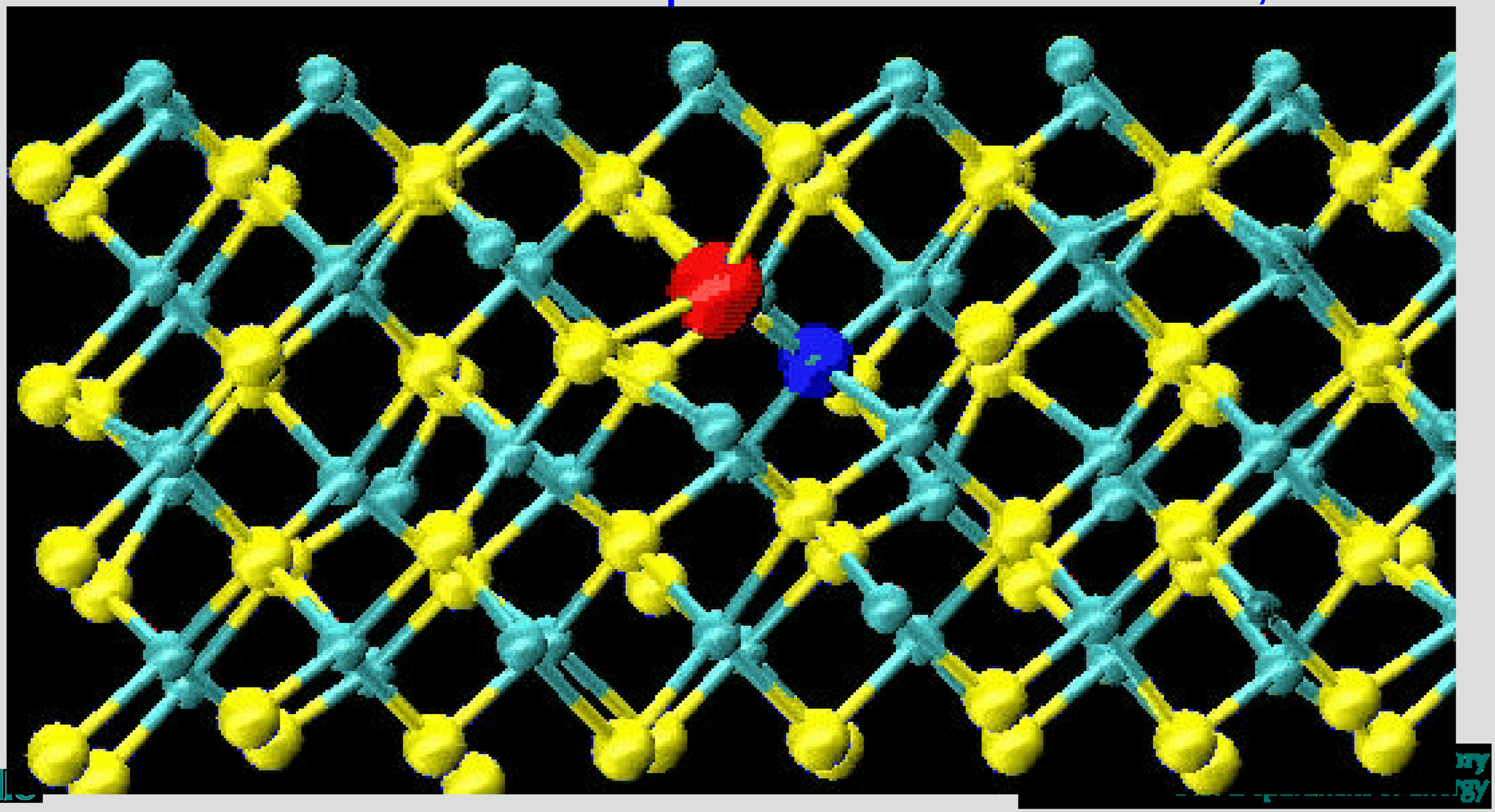

Characterizing The Electronic States Of Large Ab Initio Calculations

Defects can have several different electronic configurations. Characterizing electronic states can be a challenge in large systems that contains hundreds to thousands of molecular orbitals

Several of the possible electronic configurations of a V_C Vacancy defect in SiC

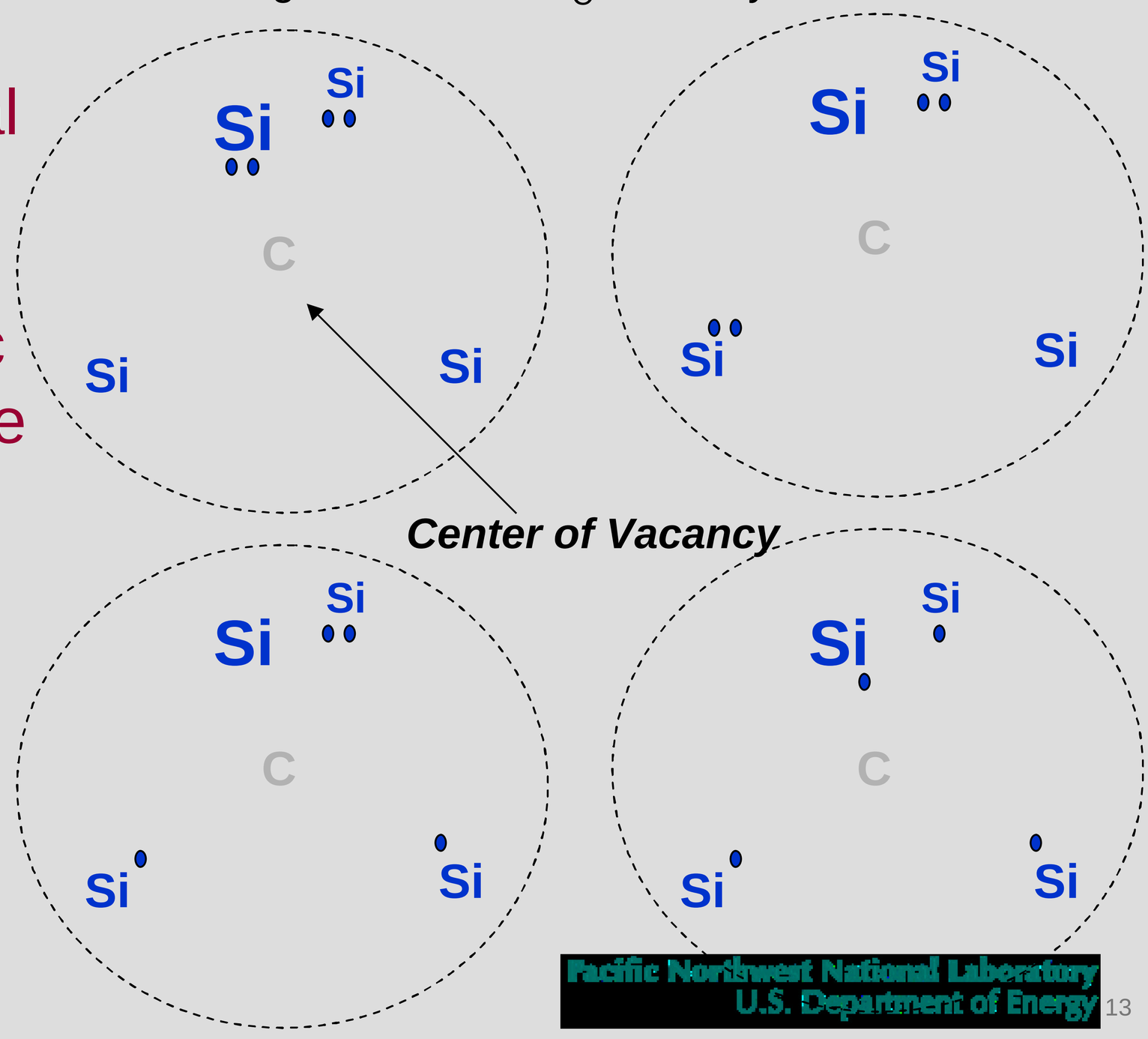

Characterizing The Electronic States Of Large Ab Initio Calculations

Ge metal Bloch orbital from LDA calculation

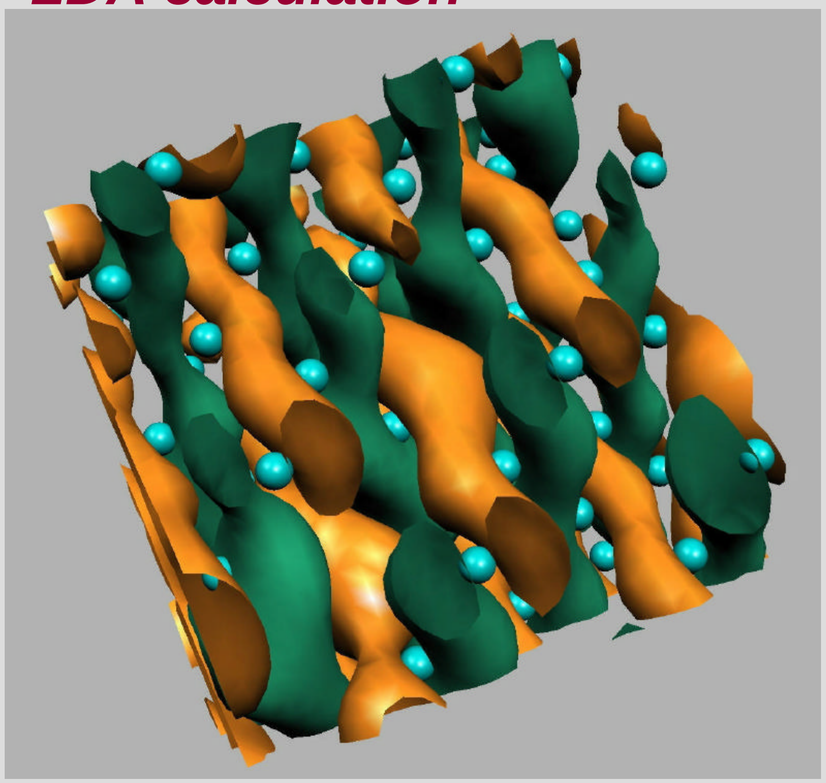

Bloch orbitals of large systems are difficult to interpret because there are a large number of them and they are delocalized over the unit cell.

Ge metal Wannier orbitals from LDA/SIC calculation

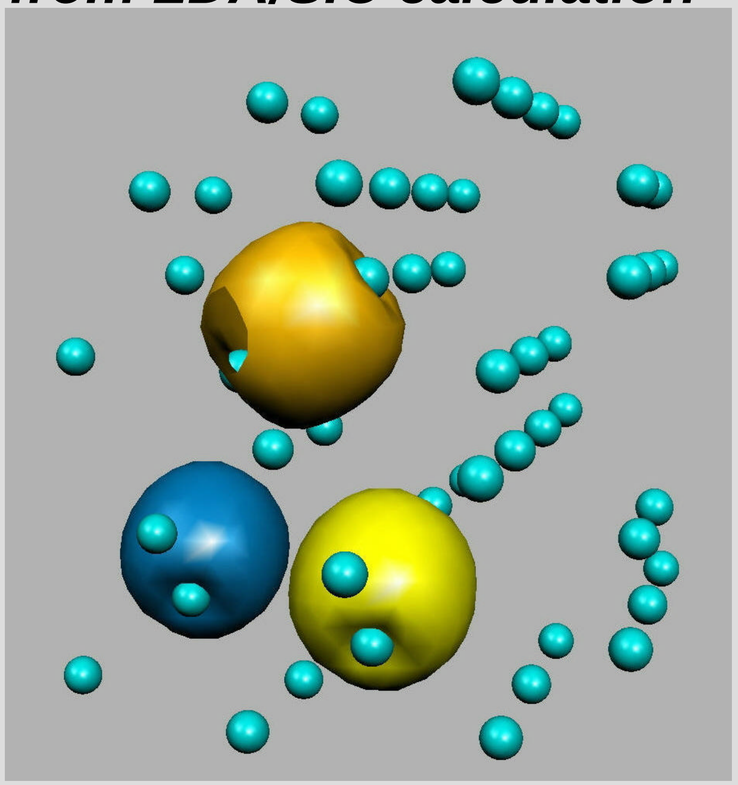

Boys (Wannier) orbitals (localized orbitals) make the interpretation of electronic states of large systems easy.

GaGa <100> Interstitial Defect in GaN

No bond found between Ga-Ga dimer

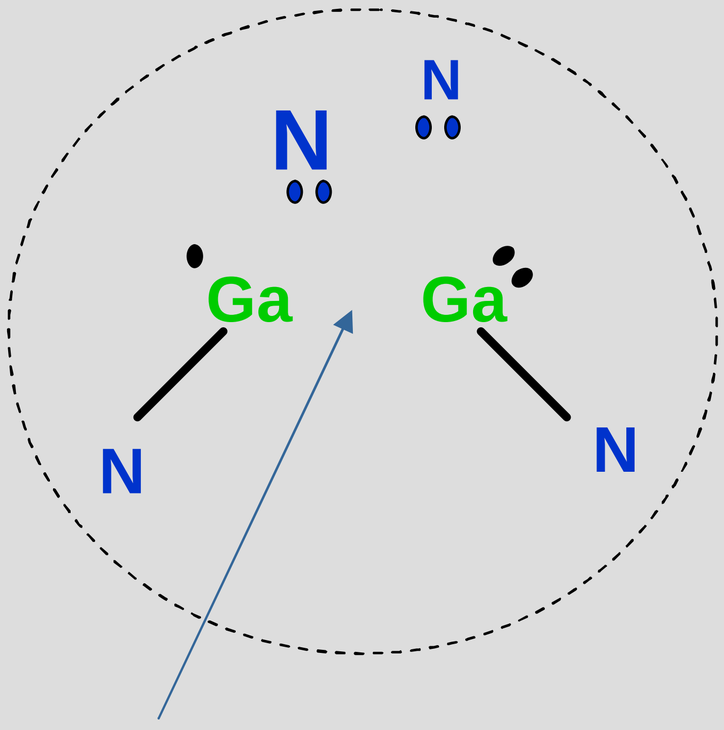

Center of Ga tetrahedral site

Ga lone pair orbitals

N lone pair orbitals

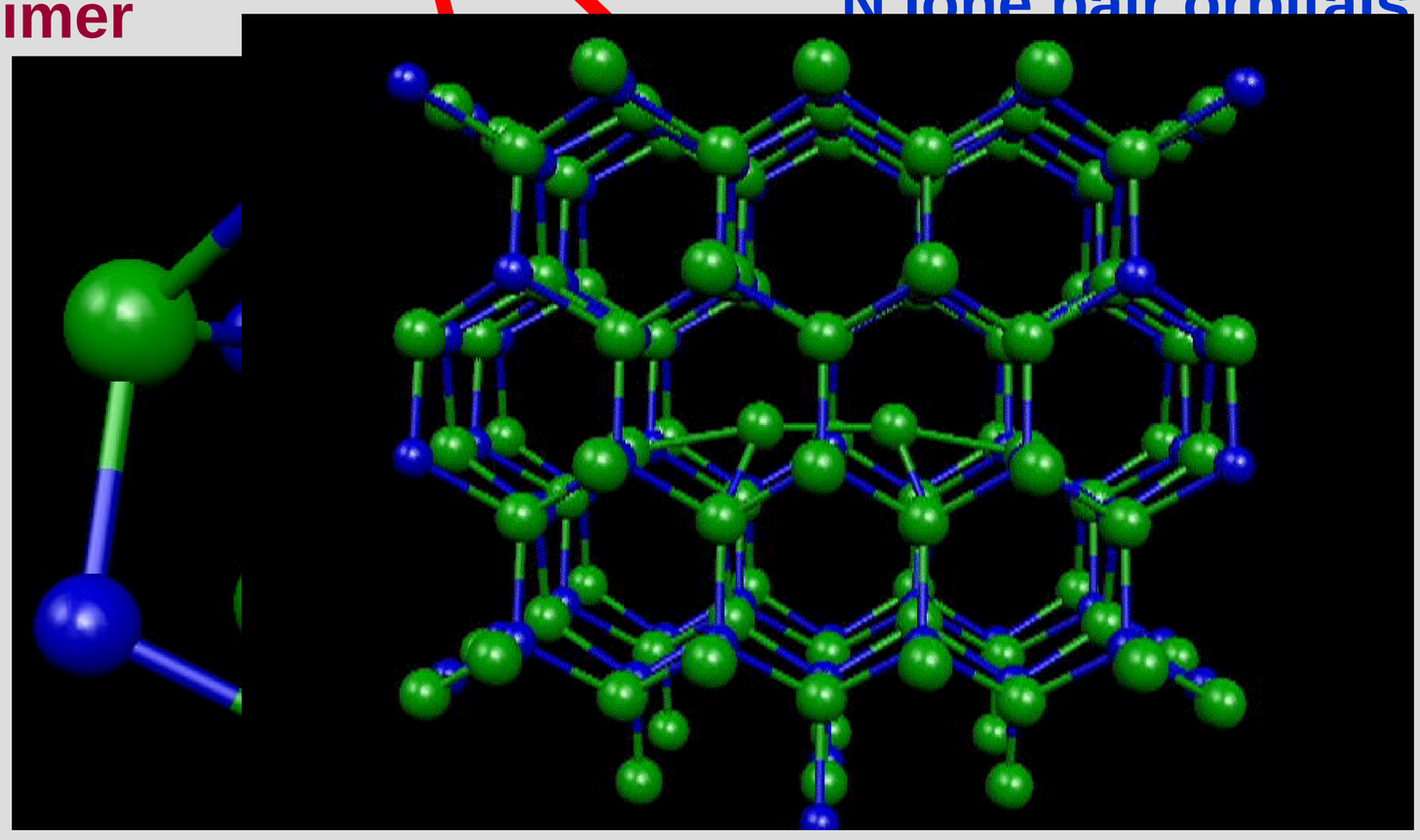

Is there a bond between Ga-Ga?

Wannier orbitals near the GaGa <100> defect

Self-Interaction in DFT

Coulomb energy contribution to the total energy of electronic system:

$$U_C = \frac{1}{2}\iint d\vec{r}d\vec{r}' \frac{\rho(\vec{r})\rho(\vec{r}')}{|\vec{r}-\vec{r}'|}$$

Where $\rho(\vec{r})$ is the total electron density: $\rho(\vec{r}) = \sum_{i=1}^{n}\rho_i(\vec{r}) = \sum_{i=1}^{n}|\psi_i(\vec{r})|^2$

Therefore, Coulomb term includes **self-interaction** of an orbital with itself:

$$U_C^{(i)} = \frac{1}{2}\iint d\vec{r}d\vec{r}' \frac{\rho_i(\vec{r})\rho_i(\vec{r}')}{|\vec{r}-\vec{r}'|}$$

In Hartree-Fock approximation, exchange interaction is evaluated exactly and self-interaction is cancelled out.

In practical implementations of DFT, exchange energy is approximated and self-interaction remains.

Total energy in DFT, Hybrid functionals, and DFT-SIC

Standard DFT:

$$E_{DFT} = \sum_{s,i} \int \Psi_{s,i}(\mathbf{r}) \left(-\frac{1}{2}\nabla^2 + V_{ext} \right) \Psi_{s,i}(\mathbf{r})\, d\mathbf{r} + \frac{1}{2} \iint \frac{r(\mathbf{r})\, r(\mathbf{r}')}{|\mathbf{r}-\mathbf{r}'|} d\mathbf{r} d\mathbf{r}' + E_{xc}[r_1, r_2]$$

DFT with hybrid XC functionals:

$$E_{HDFT} = \sum_{s,i} \int \Psi_{s,i}(\mathbf{r}) \left(-\frac{1}{2}\nabla^2 + V_{ext} \right) \Psi_{s,i}(\mathbf{r})\, d\mathbf{r} + \frac{1}{2} \iint \frac{r(\mathbf{r})\, r(\mathbf{r}')}{|\mathbf{r}-\mathbf{r}'|} d\mathbf{r} d\mathbf{r}' + a\, E_{Exch}\left[\{\Psi_{s,i}(\mathbf{r})\}\right] + b\, E_{xc}[r_1, r_2]$$

DFT-SIC Functional

Remove self-interaction in a very straightforward way (Perdew & Zunger, ’82):

$$E_{DFT-SIC}[\{r_{s,i}\}] = E_{DFT}[r(\vec{r})] - a \underbrace{\sum_{s,i} \left\{ \frac{1}{2} \int \frac{r_{s,i}(\vec{r})\, r_{s,i}(\vec{r}')}{|\vec{r}-\vec{r}'|} d\vec{r} d\vec{r}' + E_{xc}[r_{s,i}, 0] \right\}}$$

Full SIC strongly overestimates the corrections. A phenomenlogical damping factor of α=0.4 found to work well

Why Apply Hybrid Functionals (e.g. B3LYP) or Self-Interaction Corrections?

1. It can be responsible for the inability of DFT to localize spin and electron densities:
   - Size consistency problem (dissociation of $\mathbf{H_2^+}$)
   - Self-interaction (coulomb) barrier to charge or spin localization
2. If treated carefully, exact exchange or self-interaction corrections (SIC) can resolve (at least, partially) the accuracy of transition states and the band-gap problem in semiconductors and insulators.
3. When these two problems are fixed, a description of complex systems **qualitatively** different from the DFT predictions can emerge.

1. How to calculate $E_{Exch}\left[\left\{\Psi_{s,i}(\mathbf{r})\right\}\right]$?

$$E_{Exch}\left[\left\{\Psi_{s,i}(\mathbf{r})\right\}\right] = -\iint dr dr' \sum_{n(occ)}^{N} \sum_{m(occ)}^{N} \frac{\Psi_n(\mathbf{r})\Psi_m^*(\mathbf{r})\Psi_n^*(\mathbf{r}')\Psi_m(\mathbf{r}')}{|r-r'|}$$

$$\sum_{n(occ)}^{N} = \sum_{n=1}^{N} \int_{BZ} d^3k$$

This looks much more difficult than

$$E_{Coul}[r(r)] = \iint dr dr' \sum_{n(occ)}^{N} \sum_{m(occ)}^{N} \frac{\Psi_n(\mathbf{r})\Psi_n^*(\mathbf{r})\Psi_m^*(\mathbf{r}')\Psi_m(\mathbf{r}')}{|r-r'|} = \iint dr dr' \frac{r(r)\,r(r')}{|r-r'|}$$

Even for localized systems, E_{Exch} is very involved, poorly scales with the size, and is a bottleneck in applications to larger molecules or clusters.

*For **periodic** systems, $\Psi_n(r)$ are the Bloch functions, and the sums include all occupied bands as well as integration over **k-vectors.***

Bloch functions (MO) – k-space integration

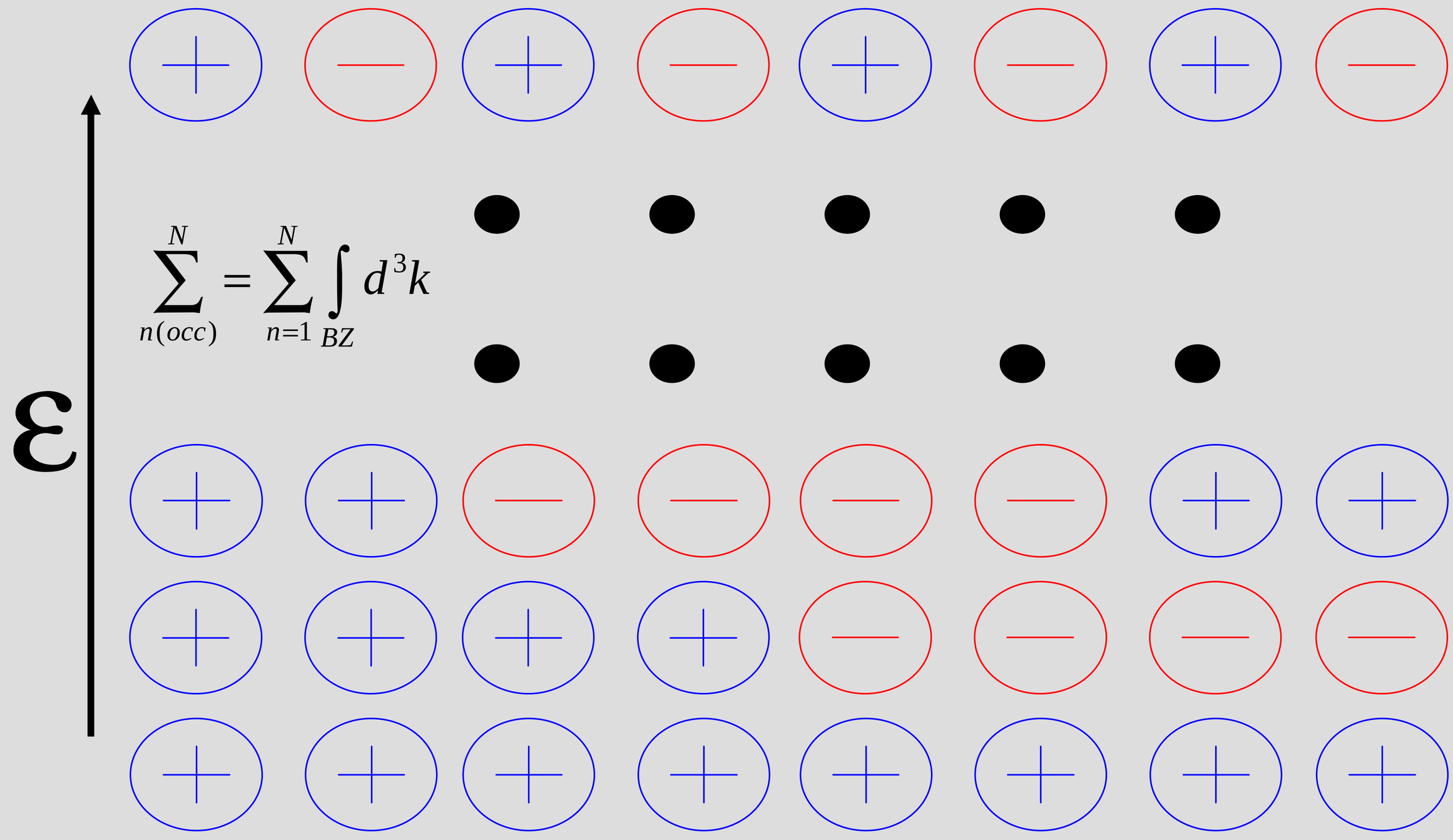

$$\sum_{n(occ)}^{N} = \sum_{n=1}^{N} \int_{BZ} d^3k$$

Wannier functions – k-space integration

Wannier functions are the result of a <u>*unitary*</u> *transformation acting on the Bloch functions, just a very special one: it acts on the space of* ***k-vectors*** *and centers* ***R*** *rather than band indices* ***n****:*

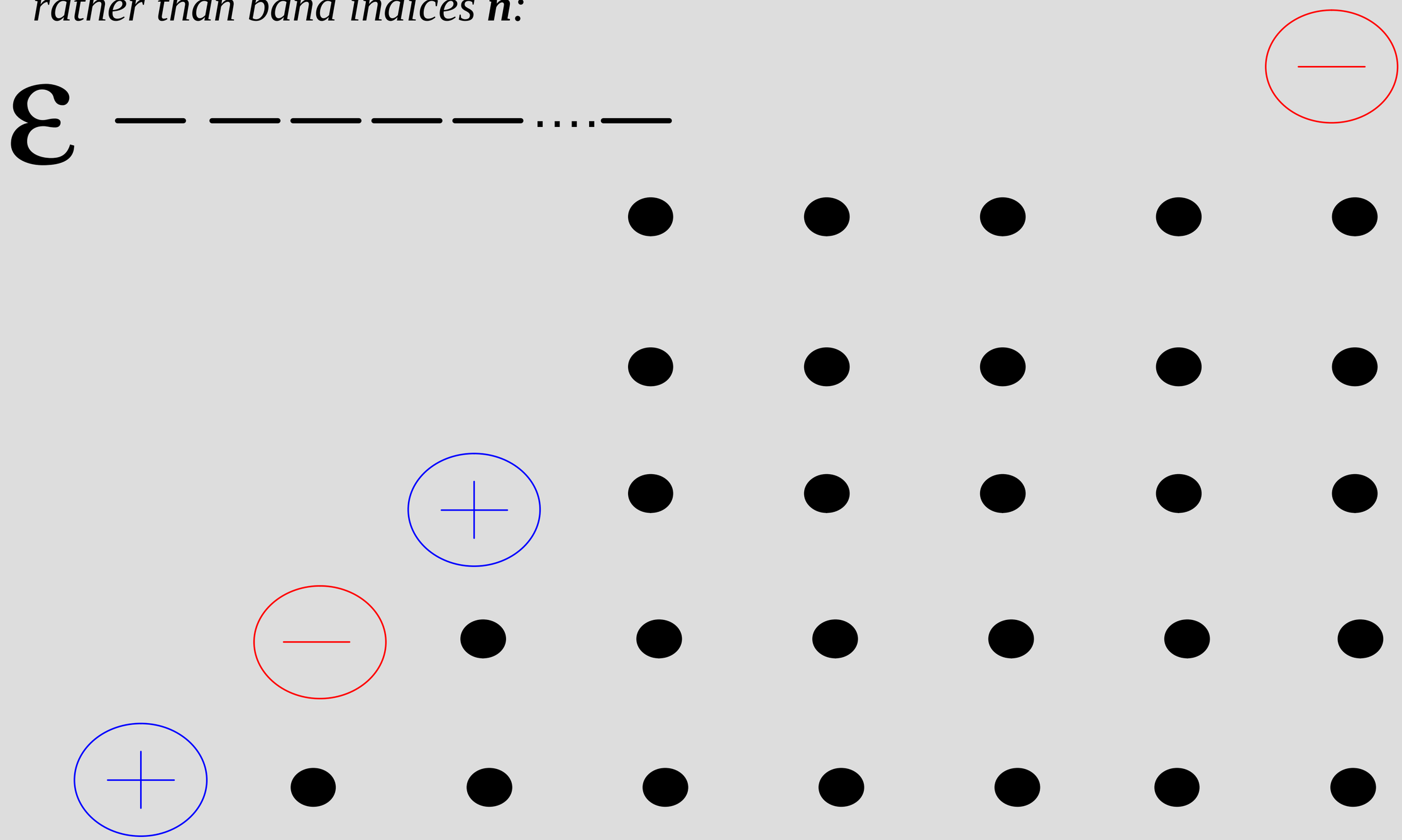

$$E_{Exch} = -\iint dr dr' \sum_{n,\mathbf{R}}^{N} \sum_{m,\mathbf{R}'}^{N} \frac{w_n(\mathbf{r}-\mathbf{R})\, w_n^*(\mathbf{r}'-\mathbf{R})\, w_m^*(\mathbf{r}-\mathbf{R}')\, w_m(\mathbf{r}'-\mathbf{R}')}{|r-r'|}$$

Why is it any better the with the Bloch functions?
*It gets better **if** each Wannier function is localized in one unit cell: then*

$$\mathbf{R}=\mathbf{R}'$$

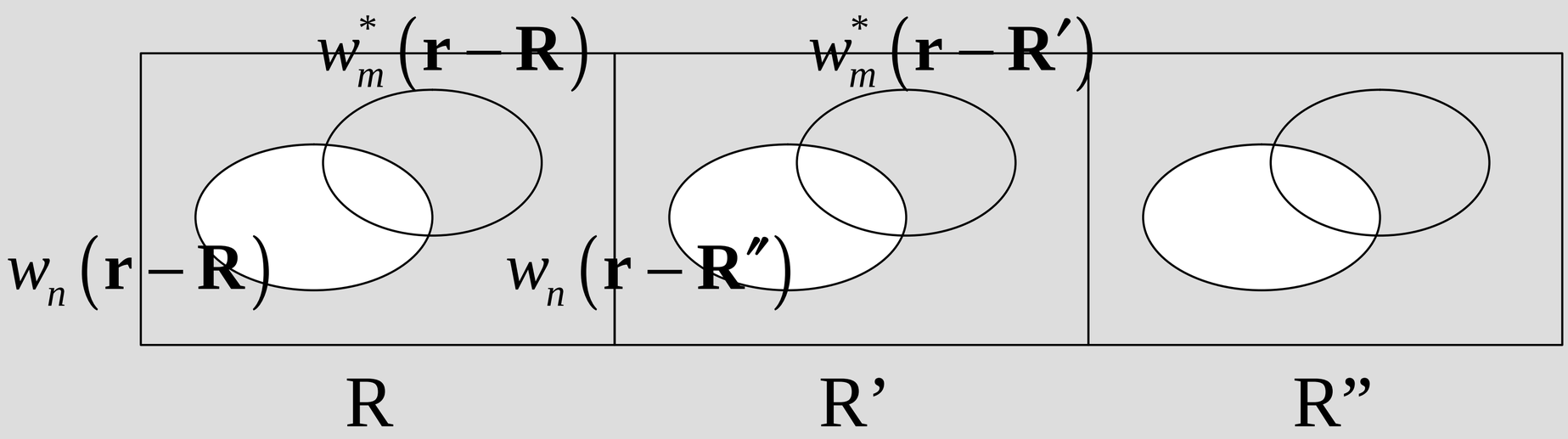

$$E_{Exch} = -\frac{1}{N}\sum_{\mathbf{R}}\iint drdr'\sum_{n}^{N}\sum_{m}^{N}\frac{w_n(\mathbf{r}-\mathbf{R})w_n^*(\mathbf{r}'-\mathbf{R})w_m^*(\mathbf{r}-\mathbf{R})w_m(\mathbf{r}'-\mathbf{R})}{|r-r'|}$$

$$= -\iint drdr'\sum_{n}^{N}\sum_{m}^{N}\frac{w_n(\mathbf{r})w_n^*(\mathbf{r}')w_m^*(\mathbf{r})w_m(\mathbf{r}')}{|r-r'|}$$

This is already much better looking. But we can do even better:

$$A_{nm}(\mathbf{r}) = w_n(\mathbf{r})w_m^*(\mathbf{r})$$

$$E_{Exch} = -\iint drdr'\sum_{n}^{N}\sum_{m}^{N}\frac{A_{nm}(r)A_{mn}^*(r')}{|r-r'|}$$

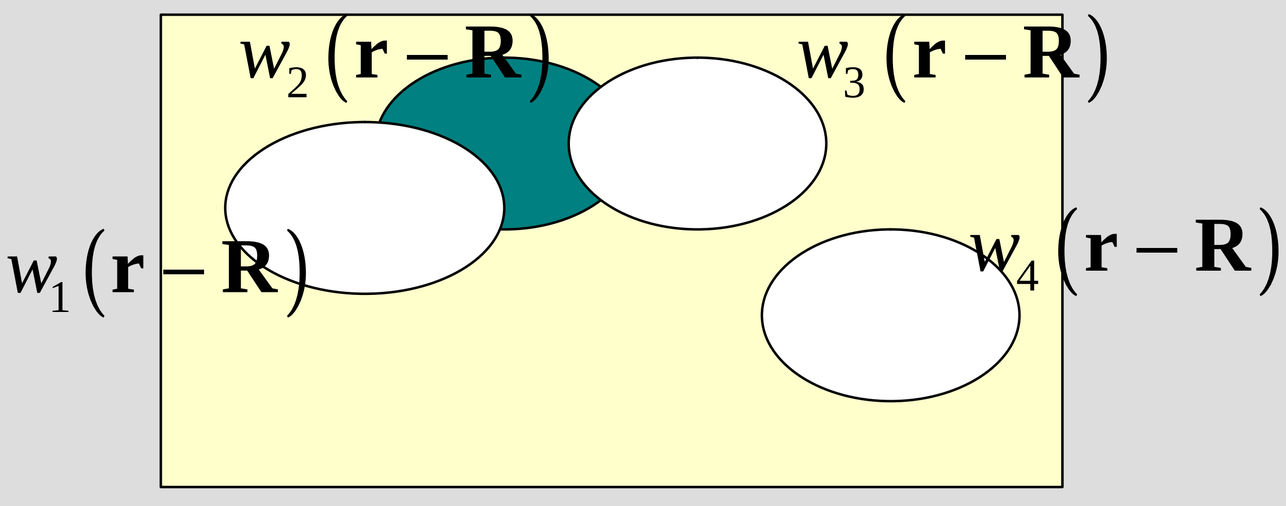

$$A_{13}(r) = A_{14}(r) = A_{24}(r) = 0$$

For the highest possible gain need ***maximally localized*** *WF's*

If *it is possible* to create localized Wannier functions for a given system

Calculating E_{Exch} with Wannier Functions

- Wannier functions constructed from single G-point Kohn-Sham Bloch states, have infinitely many artificial periodic replicas.
- To use the plane-wave method to calculate E_{Exch}, one has to limit integration to a single unit cell.

$$E_{Exch} = -\iint dr dr' \sum_{n}^{N} \sum_{m}^{N} A_{nm}(r) A_{mn}^{*}(r') f\left(\left|r - r'\right|\right)$$

To handle extended systems, we replace the Coulomb interaction by a screened Coulomb interaction:

$$f(r) = \frac{1 - \left(1 - \exp\left\{-\left(r / R\right)^{N}\right\}\right)^{N}}{r}$$

This kernel is nearly equal to $1/r$ for $r<R$ and rapidly decays to 0 for $r>R$.

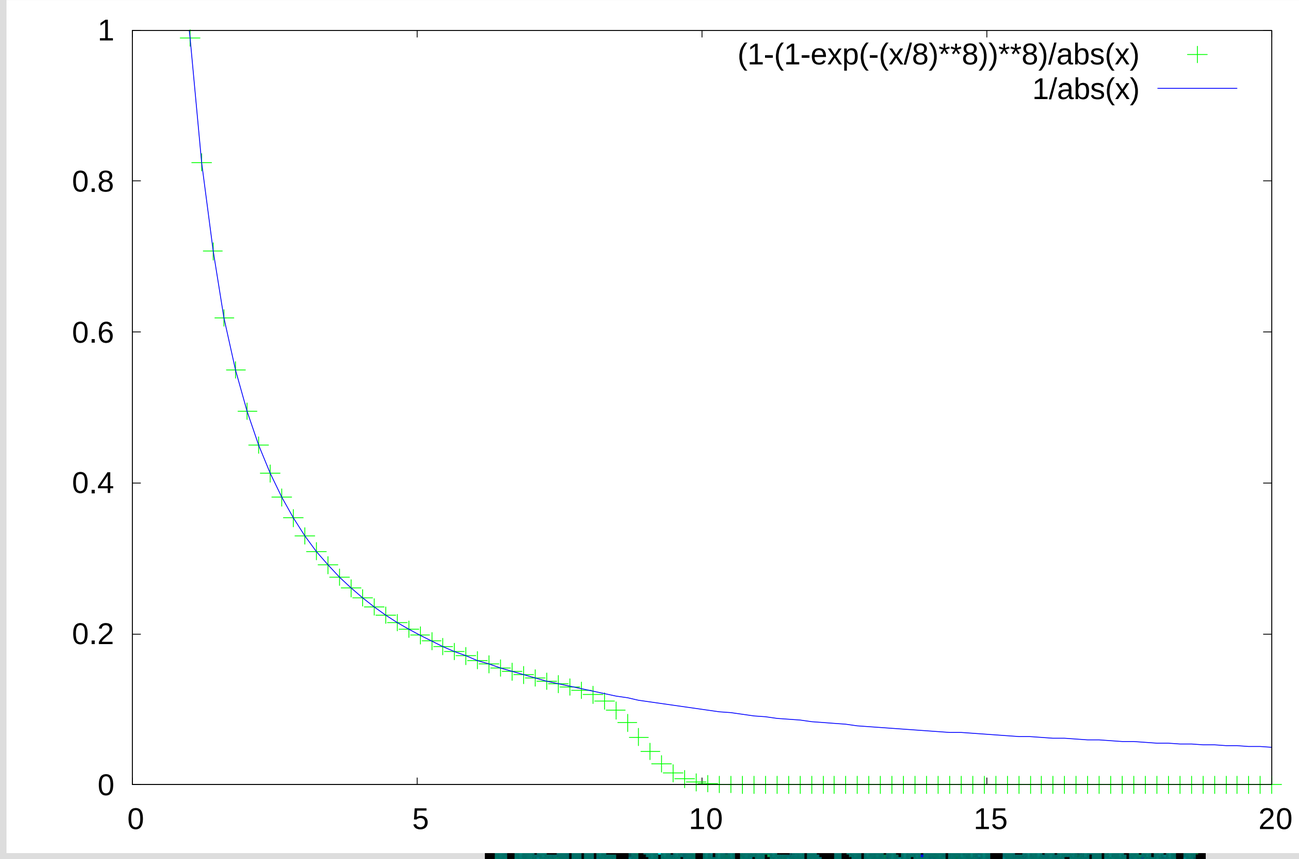

Band Gaps in Several Oxide Systems

System	Single-Particle Band Gap (eV)		
	Experiment	PBE96	PBE96-SIC
Al_2O_3	8.9	5.9	8.4
TiO_2 (rutile)	3.0	1.8	3.0
SiO_2	8.9	6.1	8.6
HfO_2	5.6	3.6	5.7
$HfSiO_4$	?	4.8	7.2
Fe_2O_3	2.1	0.8	2.3

Both DFT-SIC and Hybrid functionals can be used to correct band gap problem of DFT

System	Single-Particle Band Gap (eV)			
	Experiment	PBE96	PBE96-SIC	PBE0
Al_2O_3	8.9	5.9	8.4	8.4
TiO_2 (rutile)	3.0	1.8	3.0	3.0
SiO_2	8.9	6.1	8.6	8.7

Development of Hybrid Functionals Methods

Vacancy on 110 rutile TiO_2 surface

PBE96

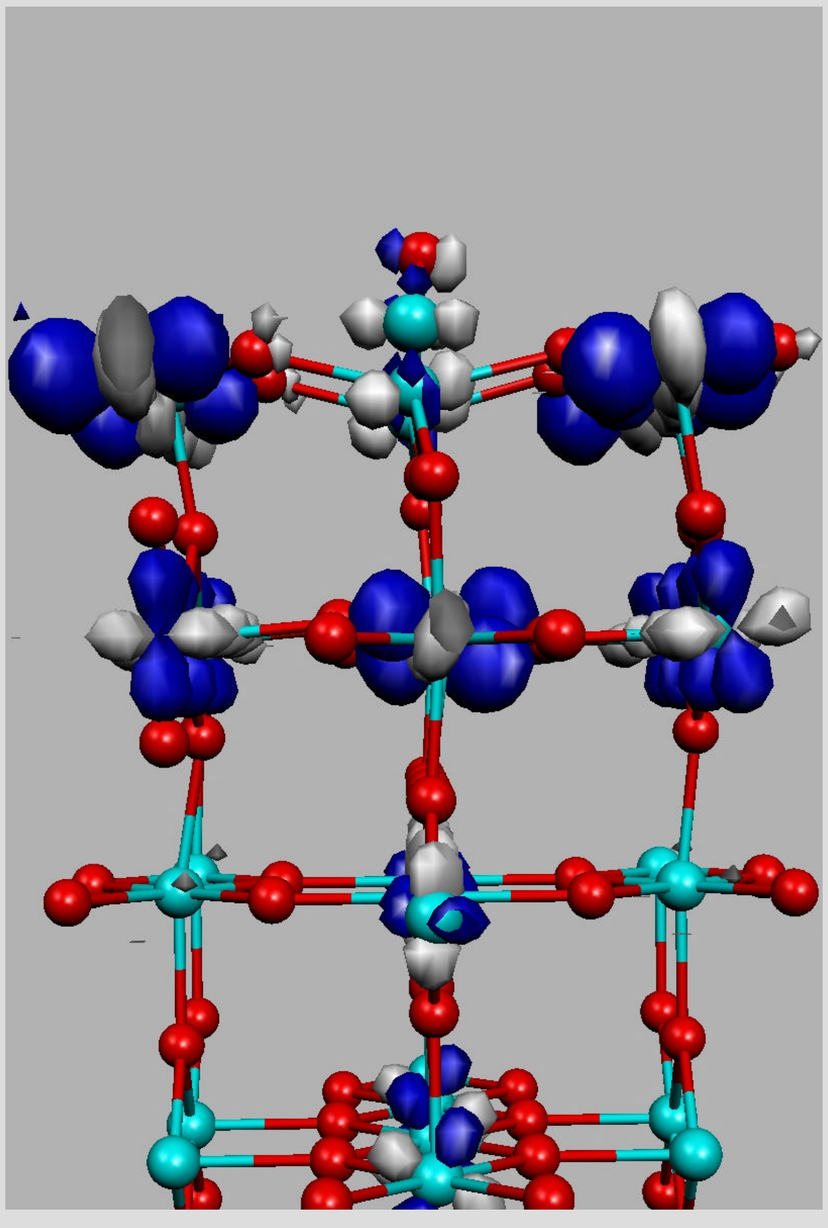

PBE0

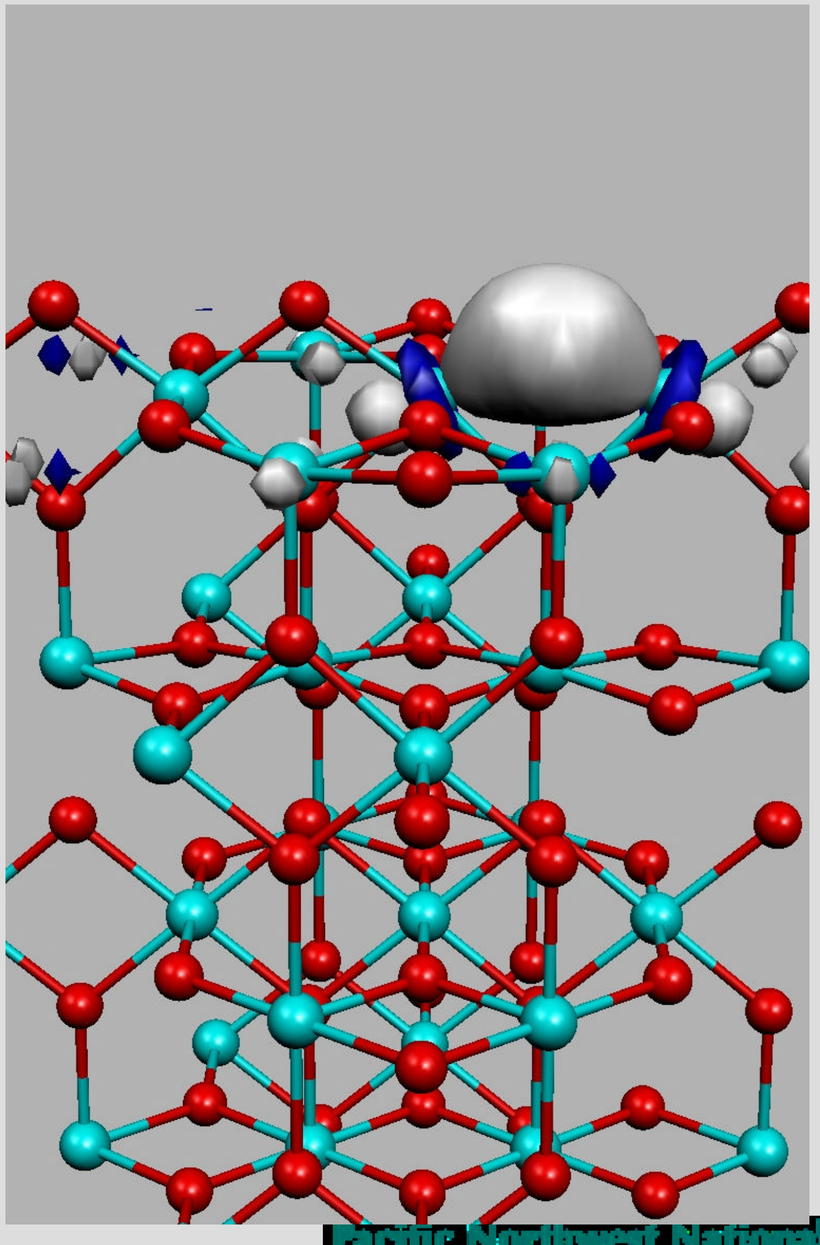

Localization of spin and charge densities by SIC

Prediction of the relative energy of localized and delocalized states is a very important issue. It is well known that DFT favors delocalized states even in the systems where charge localization is observed or expected.

(Al,Si)O_2 system: **Al** substitutional defect in silica

Experiment: Structural symmetry breaking; spin density strongly localized on a single O atom; corresponding bond is longer than the bonds with three other O atoms.

PBE96 calculation

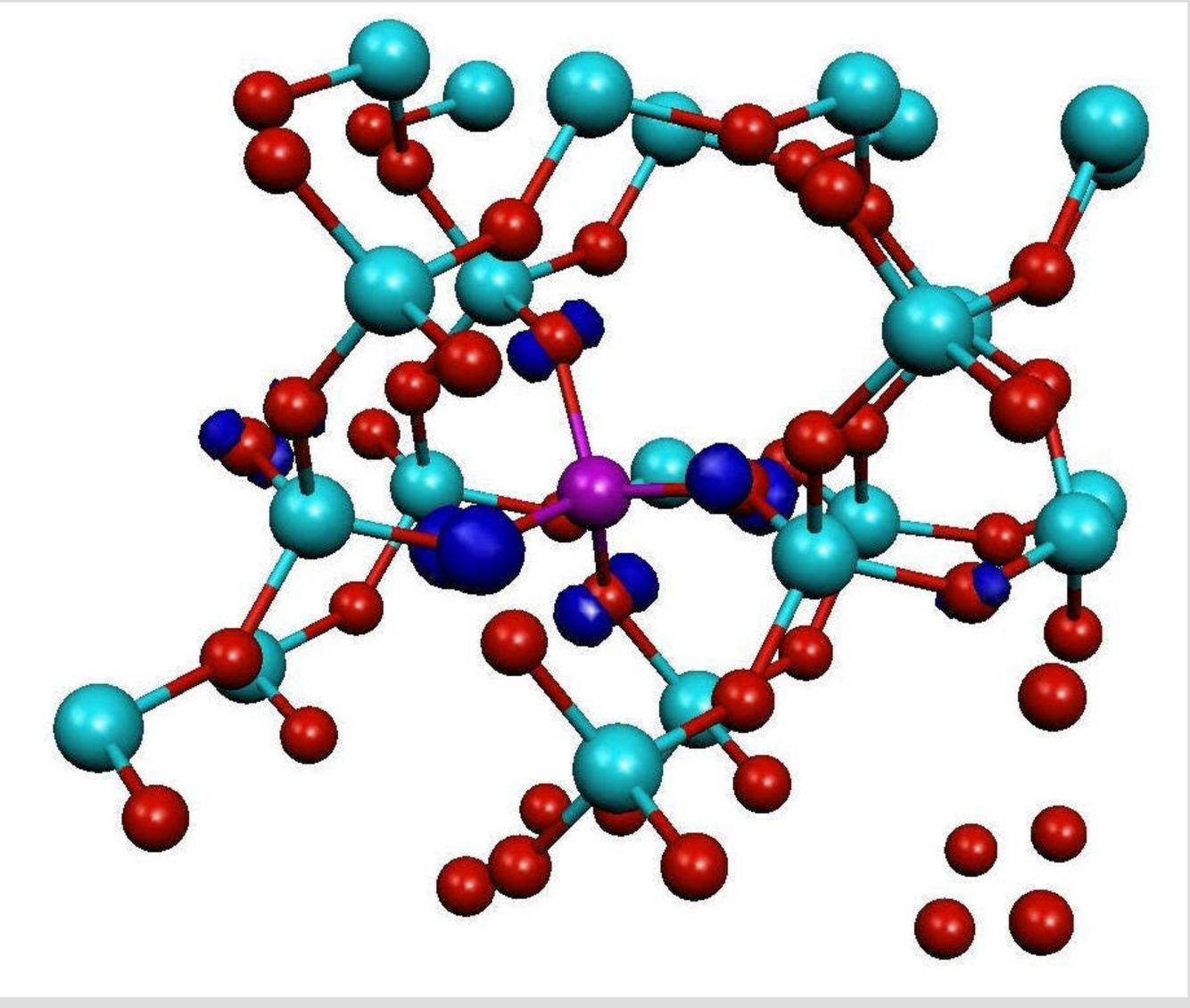

Hartree-Fock Cluster calculation

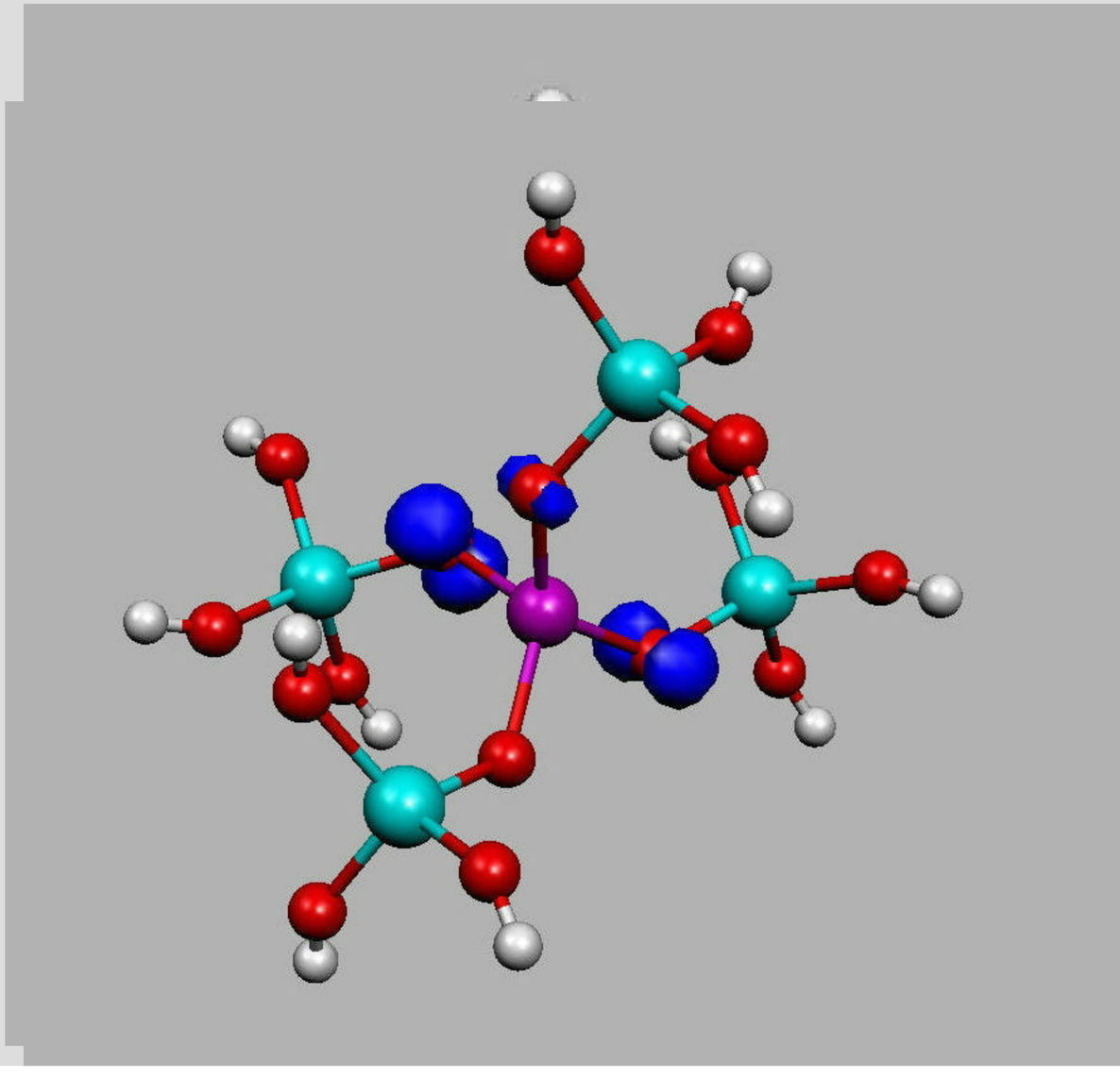

Bulk periodic system calculation with DFT - SIC

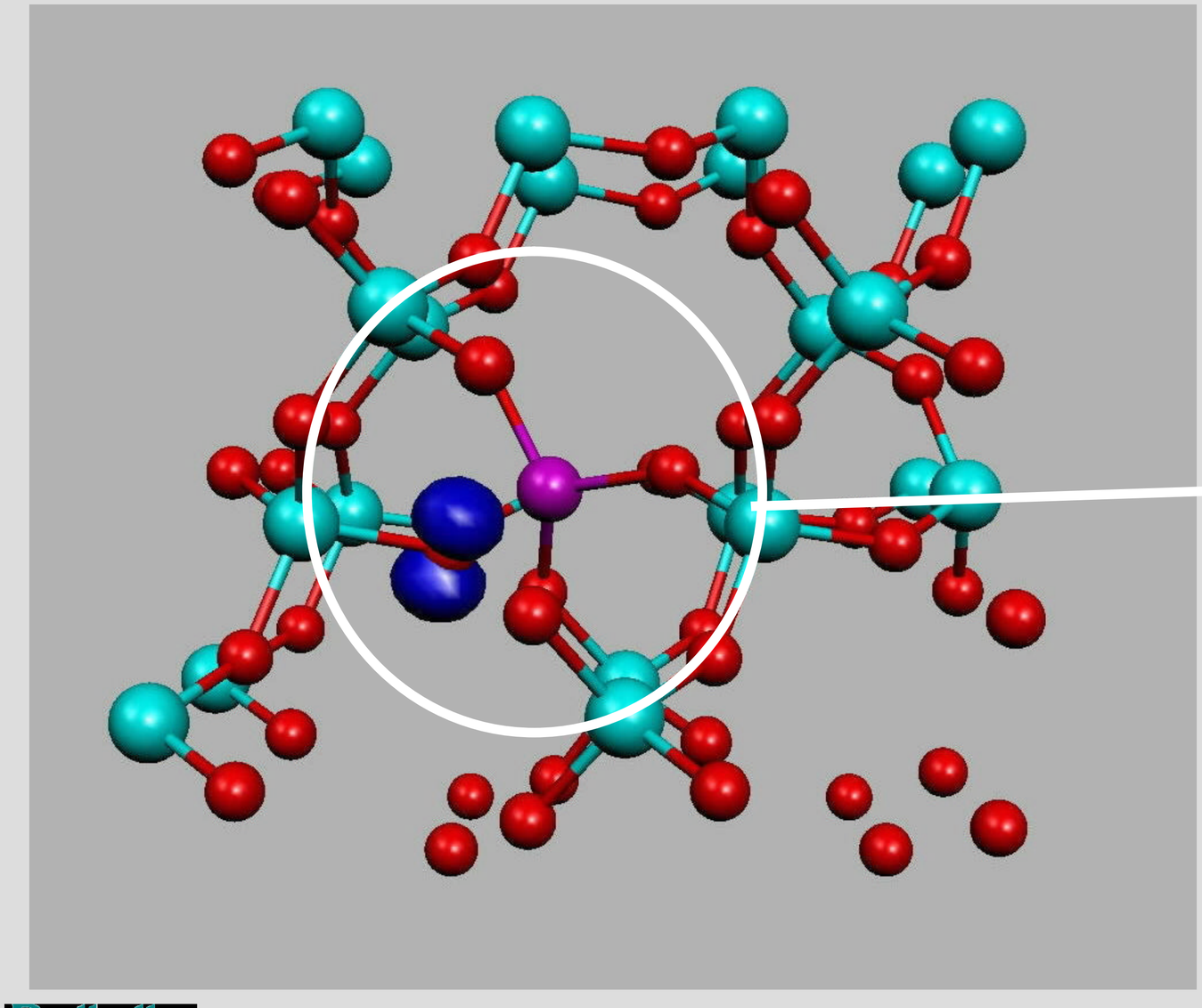

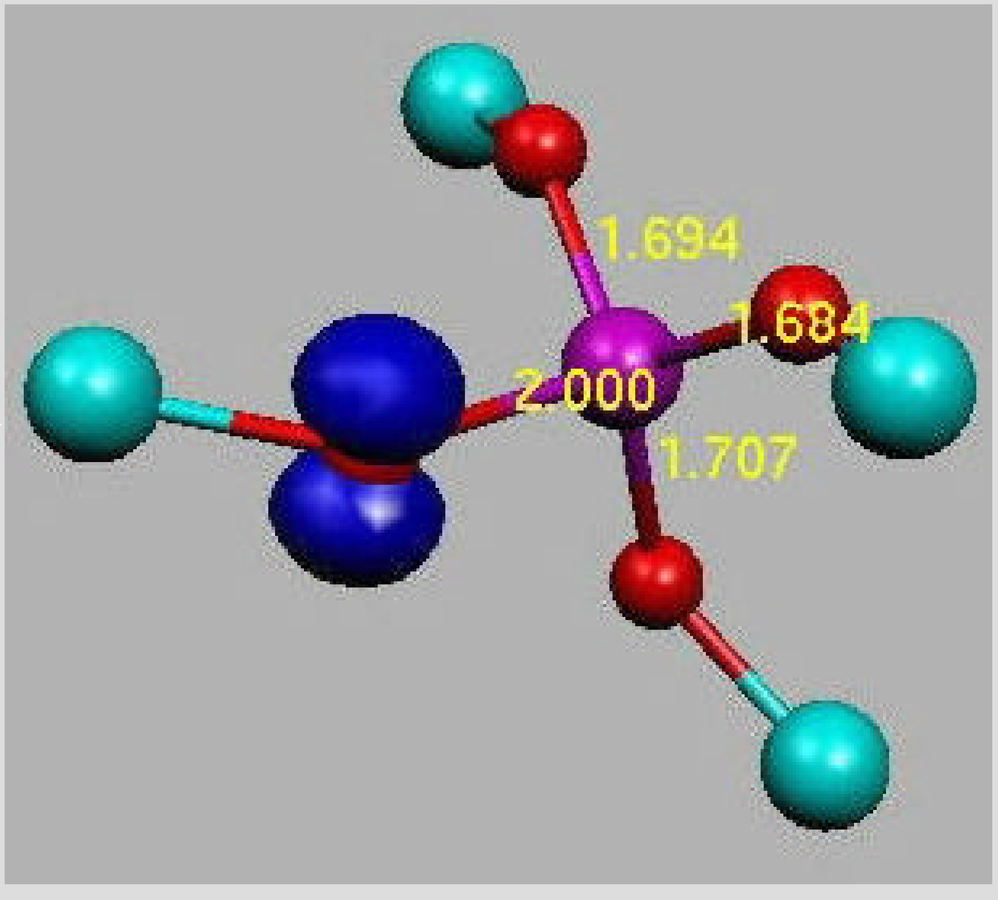

Future Directions-Adaptive classical molecular dynamics approach

- Overall dynamics is still driven by classical MD algorithm
  - enables large system size and long simulation times
- Parameters of interaction are adapted to changing conditions by means of concurrent ab-initio simulations
  - provides accurate description of chemical interactions

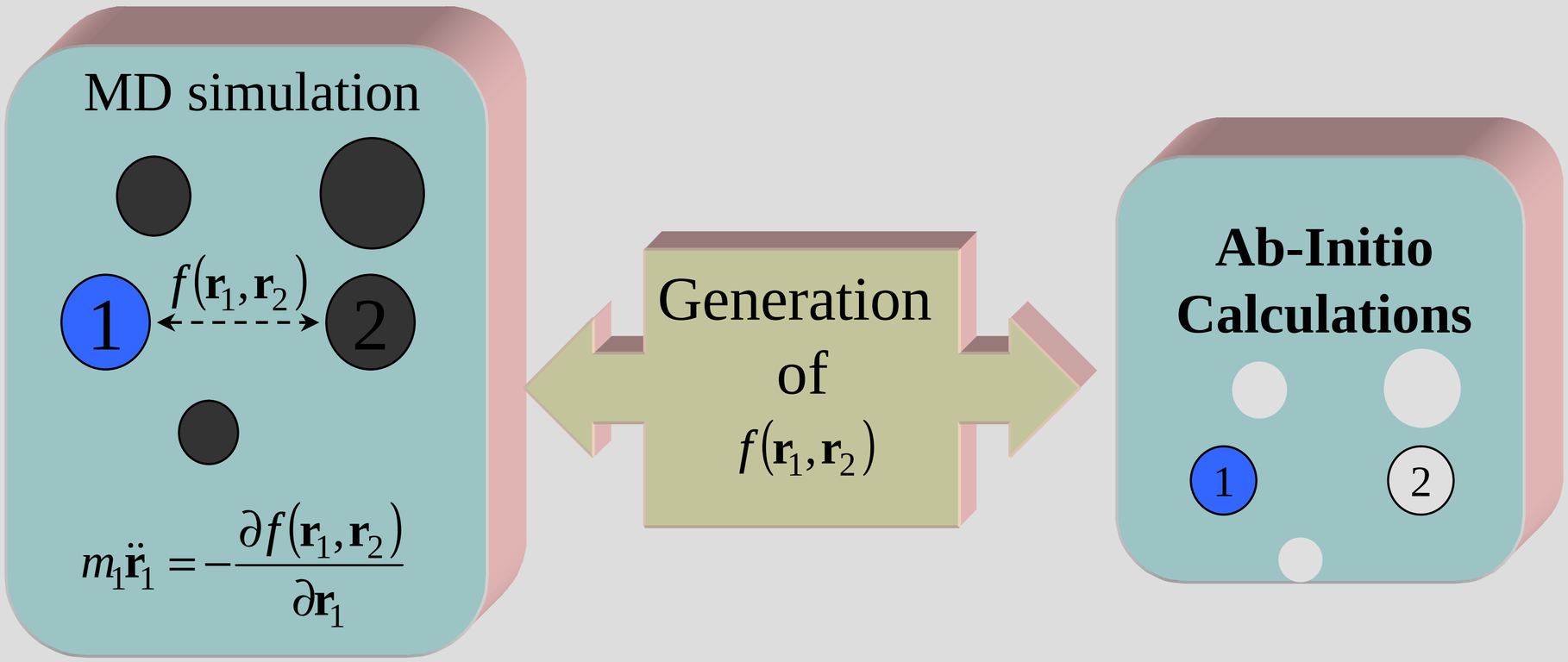

Future Directions-Traditional Approach to generating classical potentials

- No real definition of the effective classical potentials
- Procedure for its generation is not well defined
- Fitting is performed over limited number of reference configurations
- Time consuming, cannot be fully automated

Future Directions-Effective Action Approach to Classical Potentials

Rasamny, Valiev, Fernando, Phys. Rev. B 58, 9700(1998).
Valiev, Fernando, Phys. Lett. A 227, 265(1997).

- Pair-Density based representation of many-body system
- Precise definition of the effective classical potential
- “Fitting” is performed on the partition function
- Self-consistent procedure

$$W[f] = -\frac{1}{b}\ln Tr\left[\exp\left(-b\left(\hat{H} + \int f(\mathbf{r},\mathbf{r}')\hat{n}_2(\mathbf{r},\mathbf{r}')d\mathbf{r}d\mathbf{r}'\right)\right)\right]$$

$$n_2(\mathbf{r},\mathbf{r}') = \frac{dW(f)}{df(\mathbf{r},\mathbf{r}')}$$

$$\Gamma[n_2] = W[f] - \int f(\mathbf{r},\mathbf{r}')n_2(\mathbf{r},\mathbf{r}')d\mathbf{r}d\mathbf{r}'$$

$$\Gamma[n_2] = \Gamma_0[n_2] + \Gamma_{\text{int}}[n_2]$$

$$f_0(\mathbf{r},\mathbf{r}') = \frac{d\Gamma_{\text{int}}[n_2]}{dn_2(\mathbf{r},\mathbf{r}')}$$

Conclusions

1. Ab initio calculations were carried out to determine defect properties in 3C-SiC.

2. Current phenomenological (Tersoff) potentials do not predict energetic ordering of defect structures.

3. The development of more accurate potentials that match to ab initio calculations provides for more accurate MD simulations of defect migration and defect annealing processes.

4. Self-consistent DFT-SIC is implemented in the NWChem plane-wave package and can be used to study complex systems. Hybrid functionals is still under development.

5. DFT-SIC and Hybrid functionals are shown to be capable of solving *some* well-known problems of DFT .

Acknowledgements

PNNL LDRD program, DOE Office BES, Nanoscale Science, Engineering and Technology Program, DOE EMSP, Environmental Molecular Sciences Laboratory (EMSL) operations, DOE BES, Geosciences, PNNL/UW JIN, NSF. Computer time provided by EMSL MSCF facility at PNNL, and NERSC at LBL

Just re-writing the same formulas in different forms:

$$E_{Exch} = -\iint drdr' \sum_{n(occ)}^{N} \sum_{m(occ)}^{N} \frac{\Psi_n(\mathbf{r})\Psi_m^*(\mathbf{r})\Psi_n^*(\mathbf{r}')\Psi_m(\mathbf{r}')}{|r-r'|}$$

So far, collecting different pieces together

$$F(r,r') = -\sum_{n(occ)}^{N} \frac{\Psi_n(\mathbf{r})\Psi_n^*(\mathbf{r}')}{|r-r'|} \quad \text{and} \quad \sum_{n(occ)}^{N} = \sum_{n=1}^{N} \int_{BZ} d^3k$$

too much!

$$E_{Exch} = \iint drdr' F(r,r') \sum_{m(occ)}^{N} \Psi_m(\mathbf{r})\Psi_m^*(\mathbf{r}')$$

A good thing about F(r,r') is that it is ***invariant*** *with respect to rotations between the orbitals (as is, for example,* $r(r) = \sum_{n(occ)}^{N} \Psi_n(r)\Psi_n^*(r)$*).*

$$\Psi_{n,\mathbf{k}}(\mathbf{r}) \rightarrow \sum_m U_{nm}^{(\mathbf{k})} \Psi_{m,\mathbf{k}}(\mathbf{r})$$

Future Directions-Computational Implementation

$$f_0^{i+1}(\mathbf{r},\mathbf{r}') = f_0^{i}(\mathbf{r},\mathbf{r}') - a q^{i}(\mathbf{r},\mathbf{r}')$$

$$q^{i}(\mathbf{r},\mathbf{r}') = \int d\mathbf{r}_1 d\mathbf{r}_1' f_0^{i}(\mathbf{r}_1,\mathbf{r}_1')\left\{\left\langle \hat{n}_4(\mathbf{r}_1,\mathbf{r}_1',\mathbf{r},\mathbf{r}')\right\rangle - \left\langle \hat{n}_2(\mathbf{r}_1,\mathbf{r}_1')\right\rangle\left\langle \hat{n}_2(\mathbf{r},\mathbf{r}')\right\rangle\right\} - \left\{\left\langle E\hat{n}_2(\mathbf{r},\mathbf{r}')\right\rangle - \left\langle E\right\rangle\left\langle n_2(\mathbf{r},\mathbf{r}')\right\rangle\right\}$$

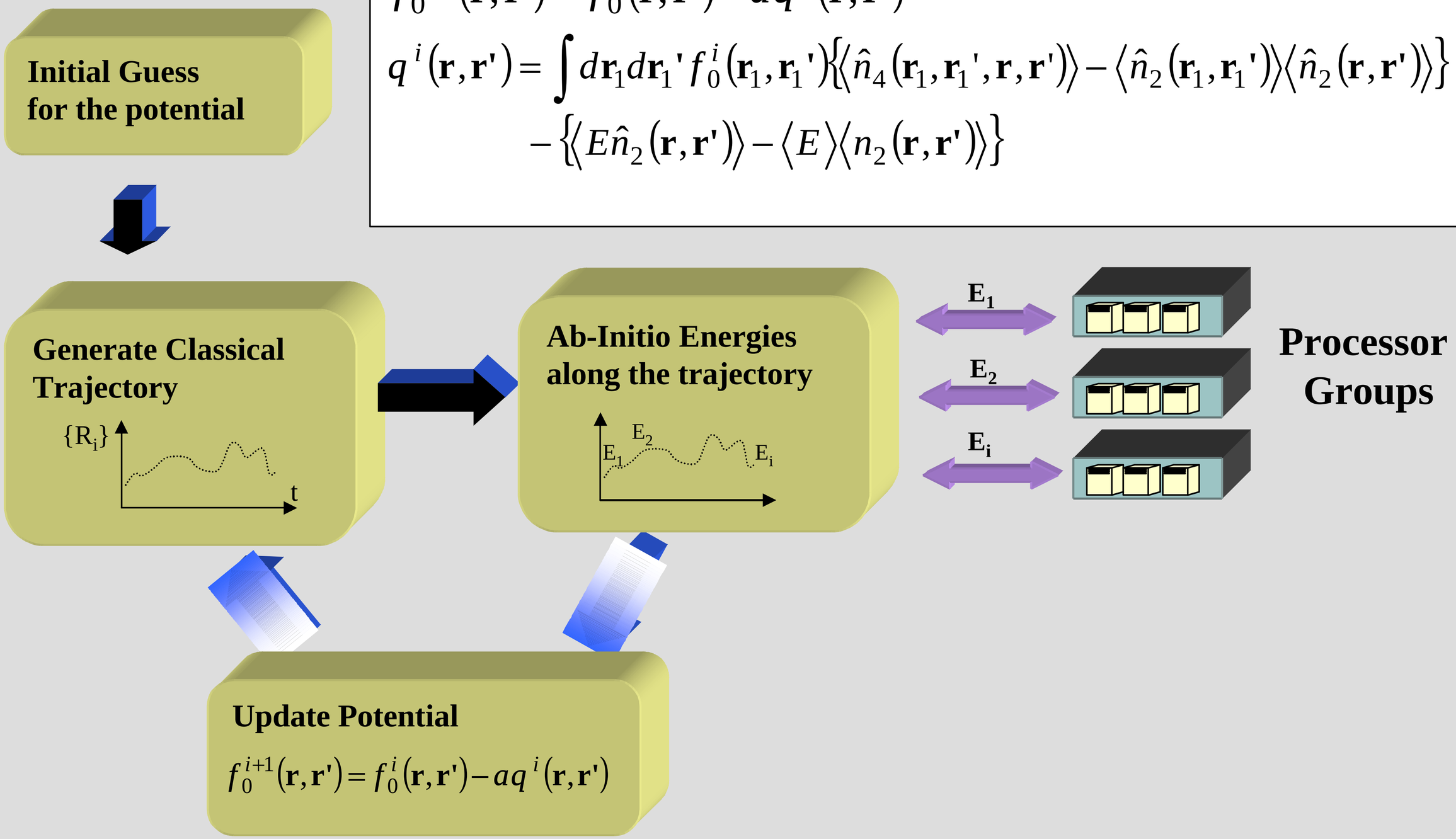

Bloch functions vs. Wannier functions

$$\Psi_{n\mathbf{k}}(\mathbf{r}+\mathbf{R}) = e^{i\mathbf{k}\mathbf{R}}\Psi_{n\mathbf{k}}(\mathbf{r})$$

$$w_n(\mathbf{r}-\mathbf{R}) = \frac{V}{(2p)^3}\int_{BZ} d^3\mathbf{k}\cdot e^{-i\mathbf{k}\cdot\mathbf{R}}\Psi_{n,\mathbf{k}}(\mathbf{r})$$

Wannier functions are the result of a <u>unitary</u> transformation acting on the Bloch functions, just a very special one: it acts on the space of ***k-vectors*** *and centers* ***R*** *rather than band indices* ***n****:*

$$w_n(\mathbf{r}-\mathbf{R}) = \frac{V}{(2p)^3}\int_{BZ} d^3\mathbf{k}\cdot U(\mathbf{R},\mathbf{k})\Psi_{n,\mathbf{k}}(\mathbf{r})$$

$AlSiO_2$ system: **Al** substitutional defect in silica. “State-of-the-art” cluster calculation imitating the bulk system (with B3LYP Functional)

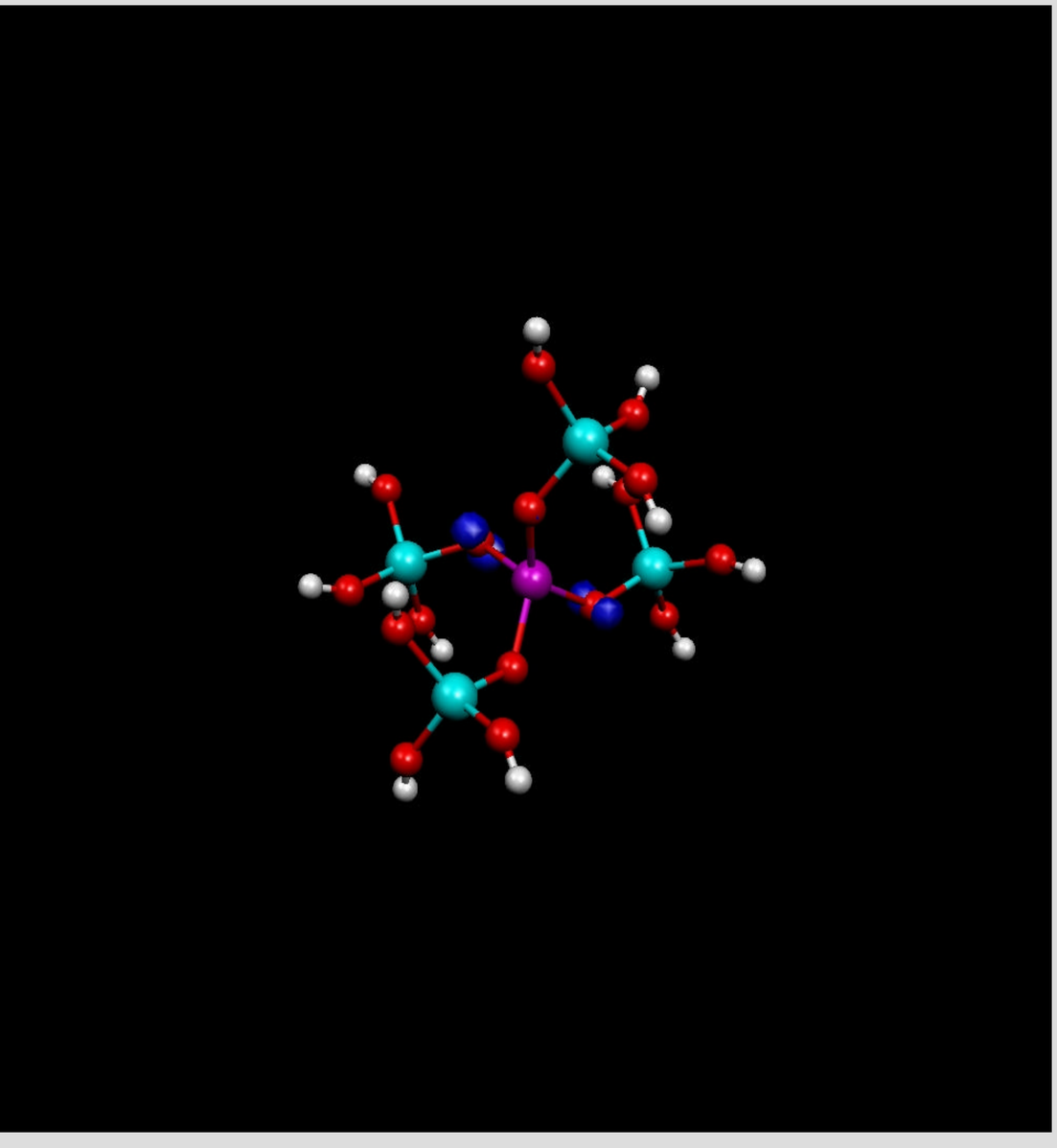

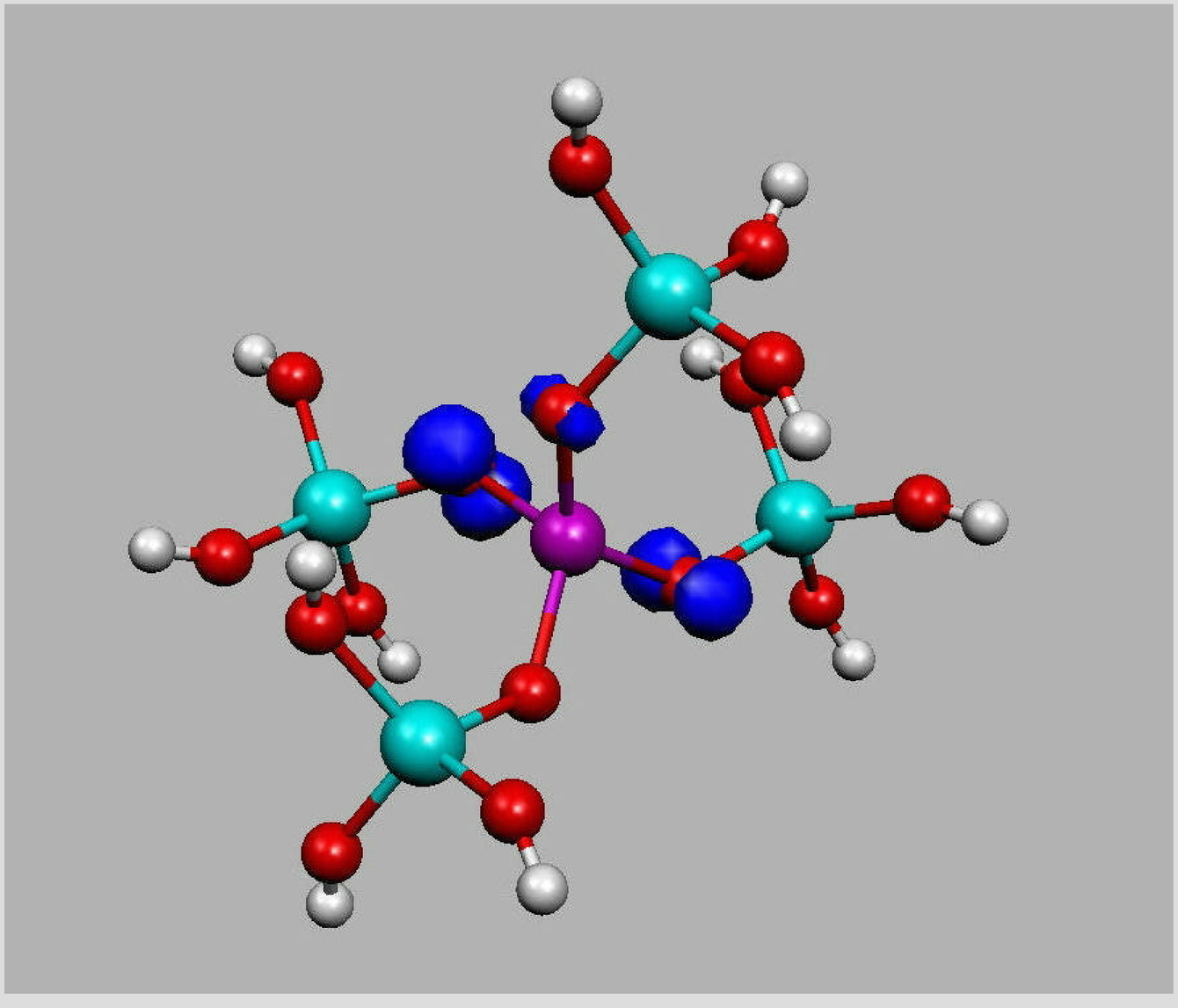

The(Kohn-Sham) one-electron orbitals in the plane-wave approach are generally delocalized Bloch states. Even for finite systems (atoms, molecules, and clusters) or Wannier states such an approach produces infinitely many periodic replicas of the system

Bloch functions (MO)

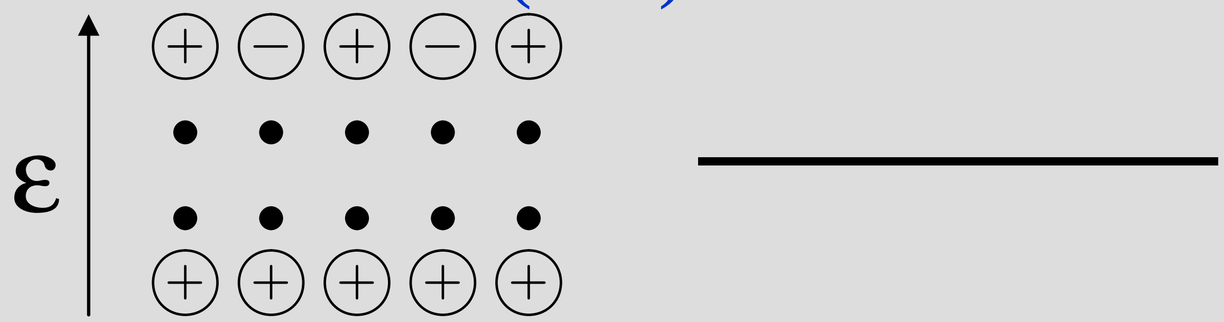

Wannier functions

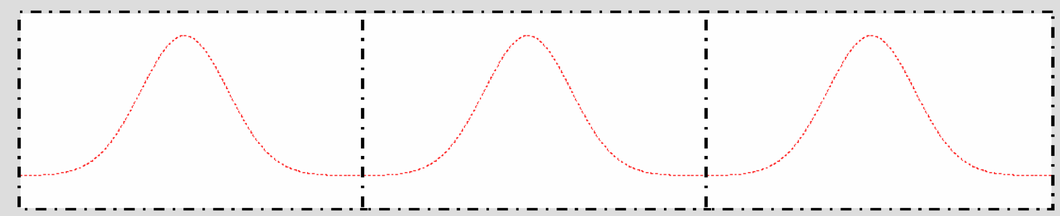

To use the plane-wave method to calculate SIC, one has to limit integration in SIC term to a single unit cell.

$$\left(E_{Coul}^{SIC}\right)_{s,i} = \frac{1}{2}\int_{\Omega}\int_{\Omega}\frac{r(\boldsymbol{r})r(\boldsymbol{r}')}{|\boldsymbol{r}-\boldsymbol{r}'|}d\boldsymbol{r}d\boldsymbol{r}'$$

For finite systems, we use aperiodic, or free-space, boundary conditions procedure developed by Bylaska et al (Bylaska et al, 1996, 2002, Valiev et al 2003) to calculate the one unit cell integral.

To handle extended systems, we replace the Coulomb interaction by a screened Coulomb interaction

$$f(\boldsymbol{r}) = \frac{1-\left(1-\exp\left\{-(\boldsymbol{r}/\boldsymbol{R})^{N}\right\}\right)^{N}}{\boldsymbol{r}}$$

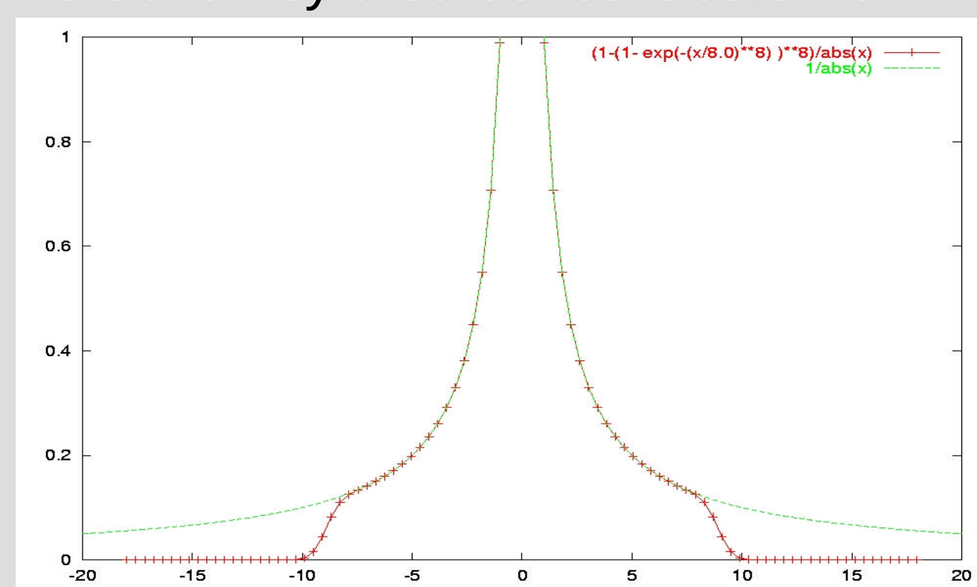

This kernel is nearly equal to 1/r for r<R and rapidly decays to 0 for r>R

Baffelle